SAPIENZA
UNIVERSITÀ DI ROMA

PhD in
Innovative Biomedical Technologies in Clinical Medicine

Study of pathogenetic molecular mechanisms and new therapeutic approaches for the treatment of Inflammatory Bowel Disease

XXXII° Ciclo
(Academic year 2018/2019)

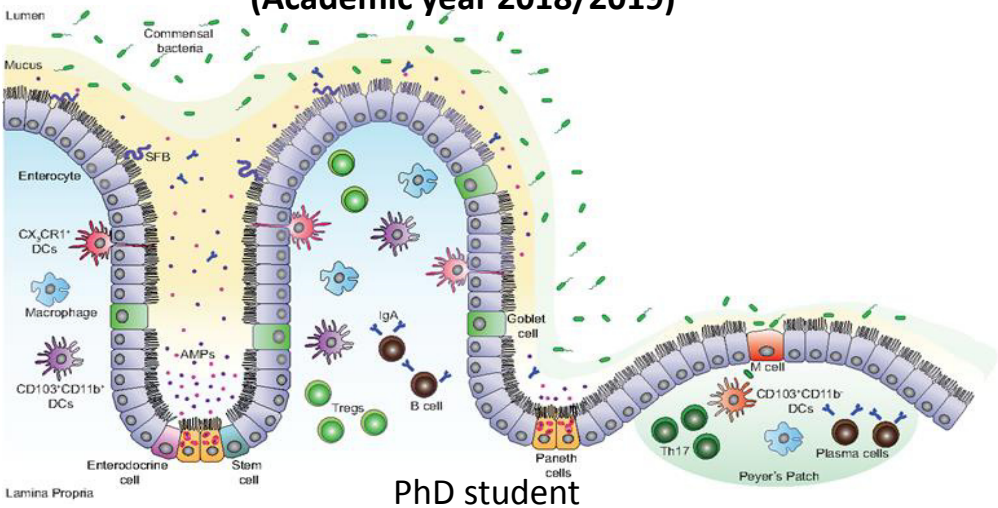

PhD student
Anna Barbara Mancuso

Supervisor
Prof.
Salvatore Cucchiara

Co-supervisor
Prof.
Laura Stronati

Co-supervisor (ENEA)
Dr.
Roberta Vitali

Sapienza University of Rome
Department of Translational and Precision Medicine

PhD in
Innovative Biomedical Technologies in Clinical Medicine

XXXII° Ciclo
(Academic year 2018/2019)

Study of pathogenetic molecular mechanisms and new therapeutic approaches for the treatment of Inflammatory Bowel Disease

PhD student
Anna Barbara Mancuso

Supervisor
Prof.
Salvatore Cucchiara

Co-supervisor
Prof.
Laura Stronati

Co-supervisor (ENEA)
Dr.
Roberta Vitali

Summary of the whole project

Inflammatory bowel diseases (IBDs), resulting from the interaction between genetic and environmental factors which influence the immune responses, are mainly divided into ulcerative colitis (UC) and Crohn's disease (CD). New studies have shown that IBD is the most common chronic inflammatory disease worldwide, affecting millions of people mainly in industrialized countries.

The number of people with IBD is increasing rapidly, thus, researchers are trying to identify new mechanisms underlying its pathogenesis and find out new treatments to cure the disease as well as to improve the general health and the quality of life of patients.

High-mobility group box 1 (HMGB1) protein, a nuclear non-histone DNA-binding protein, is released into the extracellular milieu and mediates inflammatory responses contributing to the pathogenesis of IBD.

Treatments based on antagonists specifically targeting extracellular HMGB1 have generated encouraging results in a wide number of experimental models of infectious and sterile inflammation. Interestingly, since the current therapeutic approaches for the management of IBD include drugs (immunosuppressors, steroids) and biological treatments that are often associated with adverse health consequences, the use of natural products is gaining worldwide attention.

Accordingly, the whole purpose of this study is to explore novel strategies for limiting the inflammatory potential of HMGB1. More specifically, we aimed at:

1) to assess the ability of the dipotassium glycyrrhizate (DPG), a salt of the glycoconjugated triterpene glycyrrhizin, that has been shown to inhibit the extracellular HMGB1, to reduce intestinal inflammation and improves the mucosal healing;

2) to investigate the interaction between HMGB1 and Poly (ADP-ribose) polymerase 1 (PARP1), a protein recently involved in the regulation of HMGB1 release, and explore the role of PARP1 as a novel molecular target to control gut inflammation.

The results and conclusion of the first point will be presented attaching the published original paper to the thesis (Stronati L, Palone F, Negroni A, Colantoni E, Mancuso AB, Cucchiara S, Cesi V, Isoldi S, Vitali R. Dipotassium Glycyrrhizate Improves Intestinal Mucosal Healing by Modulating Extracellular Matrix Remodeling Genes and Restoring Epithelial Barrier Functions. Front Immunol. 2019 Apr 26;10:939).

The results of the second point will be presented and discussed in this thesis.

Briefly, to induce a severe colitis, dextran sodium sulphate (DSS) was used in C57BL/6 WT or PARP1$^{-/-}$ mice. Undifferentiated and differentiated colonoid cultures of

intestinal stem cells harvested from biopsies of UC patients were treated with cytomix (TNFα + IFNγ) to induce inflammation.

Results show that PARP1$^{-/-}$ mice exhibit a less severe colitis compared to WT mice, as evidenced by the reduction of HMGB1 in the serum and stool samples. 3D colonoid cultures exposed to cytomix show increased levels of IL-1β, IL-8, TNFα and DUOXA2 as well as extracellular HMGB1. Interestingly, PARP1 specific inhibitor, PJ34, decreases the release of HMGB1 in undifferentiated as well as differentiated colonoids.

In conclusion these data demonstrate that: 1) PARP1 and HMGB1 are closely related; 2) PARP1 contributes to improve inflammation by promoting the release of extracellular HMGB1; 3) inhibition of PARP1 could represent a promising therapeutic approach to control gut inflammation.

CONTENTS

frontiers in Immunology

ORIGINAL RESEARCH
published: 26 April 2019
doi: 10.3389/fimmu.2019.00939

Dipotassium Glycyrrhizate Improves Intestinal Mucosal Healing by Modulating Extracellular Matrix Remodeling Genes and Restoring Epithelial Barrier Functions

*Laura Stronati[1], Francesca Palone[2], Anna Negroni[3], Eleonora Colantoni[2], Anna Barbara Mancuso[2], Salvatore Cucchiara[2], Vincenzo Cesi[3], Sara Isoldi[2] and Roberta Vitali[3]**

[1] Department of Molecular Medicine, Sapienza University of Rome, Rome, Italy, [2] Pediatric Gastroenterology and Liver Unit, Department of Pediatrics, Sapienza University of Rome, Rome, Italy, [3] Division of Health Protection Technologies, Territorial and Production Systems Sustainability Department, ENEA, Rome, Italy

OPEN ACCESS

Edited by:
Andrew Mark Smith,
University College London,
United Kingdom

Reviewed by:
Marco Emilio Bianchi,
Vita-Salute San Raffaele University,
Italy
Pallavi Garg,
Georgia State University,
United States

***Correspondence:**
Roberta Vitali
roberta.vitali@enea.it

Specialty section:
This article was submitted to Inflammation, a section of the journal Frontiers in Immunology

Received: 11 December 2018
Accepted: 11 April 2019
Published: 26 April 2019

Citation:
Stronati L, Palone F, Negroni A, Colantoni E, Mancuso AB, Cucchiara S, Cesi V, Isoldi S and Vitali R (2019) Dipotassium Glycyrrhizate Improves Intestinal Mucosal Healing by Modulating Extracellular Matrix Remodeling Genes and Restoring Epithelial Barrier Functions. Front. Immunol. 10:939. doi: 10.3389/fimmu.2019.00939

Gut mucosal healing (MH) is considered a key therapeutic target and prognostic parameter in the management of inflammatory bowel disease (IBD). The dipotassium glycyrrhizate (DPG), a salt of the glycoconjugated triterpene glycyrrhizin, has been shown to inhibit the High Mobility Group Box 1 (HMGB1) protein, an allarmin strongly implicated in the pathogenesis of most inflammatory and auto-immune disorders. Here we discuss new insights on how DPG acts on MH comparing the acute phase and the recovery phase from experimental colitis in mice. We found that DPG strongly accelerates MH by differently regulating pro-inflammatory (CXCL1, CXCL3, CXCL5, PTGS2, IL-1β, IL-6, CCL12, CCL7) and wound healing (COL3A1, MMP9, VTN, PLAUR, SERPINE, CSF3, FGF2, FGF7, PLAT, TIMP1) genes as observed only during the recovery phase of colitis. Relevant issue is the identification of extracellular matrix (ECM) remodeling genes, VTN, and PLAUR, as crucial genes to achieve MH during DPG treatment. Furthermore, a noticeable recovery of intestinal epithelial barrier structural organization, wound repair ability, and functionality is observed in two human colorectal adenocarcinoma cell lines exposed to DPG during inflammation. Thus, our study identifies DPG as a potent tool for controlling intestinal inflammation and improving MH.

Keywords: dipotassium glycyrrhizate, mucosal healing, DSS-induced colitis, plaur, VTN

INTRODUCTION

Inflammatory bowel diseases (IBD), are complex disorders of the gastrointestinal (GI) tract whose major phenotypes are Crohn's disease (CD), and ulcerative colitis (UC). IBD are featured by chronic inflammation which may result in irreversible mucosal damage, disability, and heightened incidence of colitis-associated neoplasias (1, 2).

Recent studies have identified gut mucosal healing (MH) as key therapeutic target and prognostic parameter in the management of IBD. Indeed, current and novel treatment options are considered and selected by their efficacy in inducing MH (3–5). The structural basis of MH is the restitution of gut epithelium that prevents translocation of commensal bacteria into the mucosa and subsequent immune-stimulation (6, 7). Achieving MH also prompts better long-term results, such as less hospitalization and surgery as well as better quality of life, with a critical impact on the natural history of the disease (8).

Intestinal cells undergoing severe inflammation release cytokines and other factors, including damage-associated molecular pattern molecules (DAMPs), that, in turn, activate inflammatory signaling pathways such as NF-κB. High Mobility Group Box-1 (HMGB1) is a DAMP prototype that normally resides in the nucleus, where it functions as a structural co-factor critical for proper transcriptional regulation in somatic cells. However, under appropriate signal stimulation, HMGB1 is released into the extracellular milieu and activates the immune system promoting inflammation (9, 10). Indeed, HMGB1 has been implicated in several inflammatory and auto-immune disorders, such as sepsis syndromes, rheumatoid arthritis, systemic lupus erythematosus and ankylosing spondylitis (11). Thus, inhibition of HMGB1 might represent a promising clinical approach for treating tissue inflammation (12, 13).

Recently, our group showed that HMGB1 is highly expressed in the inflamed intestinal tissues of CD and UC patients (14–16). Moreover, we showed that the dipotassium glycyrrhizate (DPG), a salt of the glycoconjugated triterpene glycyrrhizin (GL), a major active constituent of *Glycyrrhiza glabra* root, significantly improves the experimental colitis in mice by inhibiting HMGB1 (17).

The aims of the present study were: (1) to identify genes involved in MH pathways modulated by DPG in mice with DSS-induced acute colitis; (2) to investigate *in vitro* the outcome of DPG on MH by analyzing the impairment of epithelial cell migration, morphology, and functionality during inflammation; (3) to determine potential different effects of DPG on MH genes during a recovery phase following the DSS-induced colitis in mice; (4) to identify *in vitro* the DPG-affected genes that are crucial for efficient MH.

MATERIALS AND METHODS

Animals

C57BL/6 female mice (8–9 weeks of age; Harlan Laboratories, Udine, Italy) were housed in collective cages at 22/21°C under a 12-h light/dark cycle and with food and water provided *ad libitum*.

Induction of Acute Colitis

Mice were given 3% dextran sodium sulfate (DSS, molecular mass, 36,000–50,000 Da, MP Biomedicals, Santa Ana, CA), dissolved in autoclaved drinking water, for 7 days and then sacrificed. Mice, 8 for group, were randomly divided into three groups: (1) control group received regular drinking water; (2) mice treated with 3% (w/v) DSS; (3) mice treated with 3% DSS and 8 mg/kg/day DPG (DMG Italia Srl, Pomezia, italy), diluted in Phosphate Buffered Saline (PBS), administered by oral gavage.

Recovery After DSS-Induced Colitis

Mice, were given 3% DSS in drinking water for 5 days followed by 9 days of regular water or 8 mg/kg/day DPG, administered by oral gavage; mice were divided into the following groups (5 animals per group): (1) mice treated with DSS for 5 days and then sacrificed; (2) mice treated with DSS for 5 days, then DSS was removed and animals were treated with a vehicle (PBS) at 6, 24 (day 6), 72 (day 8), 144 (day 11), 216 (day 14) hours and then sacrificed; (3) mice treated with DSS for 5 days, then DSS was removed and animals were treated with 8 mg/kg/day DPG at 6, 24 (day 6), 72 (day 8), 144 (day 11), 216 (day 14) hours and then sacrificed.

Assessment of DSS-Induced Colitis and Histological Score

Animals were daily examined and the clinical score (CS) was assessed by evaluating stool consistency (0 for normal stool, 1 for moist/sticky stool, 2 for soft stool, 3 for diarrhea), presence of blood in stools (0 for no blood, 1 for evidence of blood in stools or around anus, and 2 for severe bleeding) and general appearance of the animal (0 was assigned if normal, 1 for ruffled fur or altered gait, 2 for lethargic or moribund), according to Maxwell et al. (18). Mice were daily weighed, and the percentage of weight loss was calculated in relation to the starting weight. The 7th day, animals were euthanized, colon removed and examined for weight and length. Distal colonic specimens were frozen in liquid nitrogen and stored at −80°C for further analyses. For histological analysis, samples were fixed immediately in a 10% (w/v) formalin solution and embedded in paraffin, sectioned (4 μm thickness), mounted on glass slides. Slices were stained using standard hematoxylin and eosin (H&E) techniques. Samples were analyzed by light microscopy and scored according to Maxwell et al. (18).

Ethic Statement

Experimental procedures were previously approved by the Ministry of Health and the study was carried out in accordance with the Italian regulations on animal welfare. The protocol was approved by the Committee on the Ethics of Animal Experiments of the Italian National Agency for New Technology, Energy and Sustainable Economic Development (ENEA-Permit Number: 1175/2016-PR).

RT2 Profiler PCR Array on Genes of Wound Healing Pathway

Total RNA was isolated from mouse colonic tissues using the RNeasy Microarray tissue kit (Qiagen), and 1 μg of total RNA was reverse transcribed by the RT2 First Strand Kit (Qiagen). Samples were analyzed by a RT2 Profiler PCR array (Qiagen) to evaluate the expression levels of a panel of 84 genes central to MH response. Gene list: *Extracellular Matrix (ECM) and Cell Adhesion Molecules:* ECM Structural Constituents: COL14A1, COL1A1, COL1A2, COL3A1, COL4A1, COL4A3, COL5A2, VTN; ECM Remodeling Enzymes: Cathepsin

G, Cathepsin K, Cathepsin V, F3 Coagulation Factor III, F13A1, FGA, MMP1, MMP2, MMP7, MMP9, PLAT, PLAU, PLAUR, PLG, PAI-1 (SERPINE), TIMP1; Cell Adhesion Molecules: CDH1, ITGA1, ITGA2, ITGA3, ITGA4, ITGA5, ITGA6, ITGAV, ITGB1, ITGB3, ITGB5, ITGB6; Cytoskeleton Regulators: RAC1, ACTA2 (α-SMA), ACTC1, TAGLN; *Inflammatory Cytokines and Chemokines:* C-C motif chemokine 7, CCL12 (MCP-1), CD40LG (TNFSF5), CXCL1, CXCL11, CXCL2, IFNG, IL-10, IL-1B, IL-2, IL-4, IL-6, MIP-2BETA (CXCL3); *Growth Factors:* CTGF, ANGPT1, GM-CSF (CSF2), CSF3 (GCSF), FGF2, FGF7, FGF10, HGF, IGF1, MIF, TGFA, TGFB1, TNF, PDGFA, VEGFA; *Signal Transduction:* TGFβ Signaling: TGFB1, STAT3; WNT Signaling: CTNNB1, WISP1; Kinases: ERK2, MAPK3, PTEN; Cell Surface Receptors: EGFR, IL6ST (GP130); *Other Signal Transduction Genes*: PTGS2 (COX2); A threshold of 3.5 times was chosen.

The normalization and all the data analysis were performed according to the manufacturer's instructions using their web-based software package: https://dataanalysis.qiagen.com/pcr/arrayanalysis. For the normalization it uses the average of five housekeeping genes: Actb, B2m, Gapdh, Gusb, Hsp90ab1. In order to identify false positives a statistical assessment of the False Discovery Rate were carried out by Benjamini–Hochberg procedure with critical value of 0.05 (http://www.biostathandbook.com/multiplecomparisons.html).

Cell Lines

Caco2 and HT29 (HTB38, CL.19A) (human colorectal adenocarcinoma cell lines) were purchased from American Type Culture Collection (ATCC, Rockville, MA, USA). Caco2 and HT29 were maintained at 37°C, 5% CO_2, in Dulbecco's minimum essential medium (DMEM, Gibco, Life Technologies, Carlsbad, CA, USA) and McCOY's 5A medium (Gibco), respectively, supplemented with 10% inactivated fetal bovine serum (FBS Eu Approved, Euroclone, Milan, Italy), 2 mM L-Glutamine, 100 U/ml penicillin and 100 μg/ml streptomycin (Euroclone). Caco2 were differentiated in culture medium for 16 days.

Real Time-PCR

Total RNA was isolated from mouse colonic tissues using the mini RNeasy kit (Qiagen), and 1 μg of total RNA was reverse transcribed by IScriptTM cDNA Synthesis Kit (BioRad, Hercules). The RT-PCR amplifications were obtained by a BioRad CFX96 TouchTM Real-Time PCR Detection System using SsoAdvanced Universal SYBR Green super Mix (BioRad).

The primers used were summarize in **Table 1**. The expression level of each mRNA was assessed using the standard curve method and *GADPH* was used for normalization.

Immunoblot Analysis

Mouse colonic tissues were suspended in ice-cold lysis buffer (50 mM Tris (pH 7.4), 5 mM EDTA, 250 mM NaCl, 0.1% Triton X-100, 1 mM phenylmethylsulfonyl fluoride, 5 mg/ml aprotinin, 5 mg/ml leupeptin, and 1 mM sodium orthovanadate (Sigma), homogenized and incubated in ice for 30 min. Samples were centrifuged at 14,000 r.p.m. for 10 min., supernatants collected and analyzed by western blot.

Ten microgram of total proteins, were fractionated by sodium dodecyl sulfate-polyacrylamide gel electrophoresis to detect selected MH proteins. Proteins were transferred in polyvinylidene fluoride membrane (Bio-Rad) and blocked with TBS-T (Tris-buffered saline with Tween-20) containing 5% non-fat dry milk. Anti-MMP9 (1:1,000; NovusBio), anti-VTN (1:1,000; NovusBio), anti-COL3A1 (1:1,000; ThermoScientific), anti-TIMP1 (1:1,000; Bioss), anti-PLAUR (1:1,000; Origene), and anti-β-actin (1:5,000; Sigma) antibodies were diluted in TBS-T containing 3% non-fat dry milk and incubated overnight at 4°C. Membranes were washed in TBS-T, incubated for 1 h with horseradish peroxidase-conjugated secondary antibody (Santa Cruz Biotechnology Inc.,), washed in TBS-T, and developed with ECL-Plus (GE Healthcare, Life Science). Densitometrical analyses of the blots were performed using the Software ImageQuant (GE Healthcare, Life Science).

Wound Healing Assay

Wound Healing Assay was assessed by scratch test as previously described (19). HT29 cells were cultured in 6-well plated at a density of 2×10^5 cells/ml until confluence reached 90%. A straight-line wound was made using a 10-ul pipette tip. Cell debris and smoothed the edge of the straight-line wound were removed by a wash with PBS and cells were then maintained in a medium with a reduced percentage of FBS (1%). Then cells were exposed to cytomix [TNFα (100 ng/ml) and INFγ (250 ng/ml), Peprotech, Rocky Hill, USA] or to B-box (10 μg/ml) (HMGBiotech, Milan, Italy) in presence or absence of DPG (300 μM) or anti-HMGB1 antibody (Sigma) for 48 h. In a second set of experiments, cells were treated with cytomix for 24 h and then were exposed to DPG (300 μM, Sigma), anti-VTN (1:1,000) and anti-PLAUR (1:1,000), alone or in combination, for 24 h. In both case, cells migrated into the wounded area were visualized at 0, 6, 24, and 48 h by Hematoxylin and Eosin staining. Images of each condition were acquired at a magnification of 10X. Cellular density related to a fixed wounded area (1 mm^2) was measured after 48 h using ImageJ software (available in the public domain at www.nih.gov; National Institutes of Health [NIH], Bethesda, MD, USA) (10 acquisition for each experimental point). The experiment was replicated three times.

Immunofluorescence

Cells exposed to cytomix or co-exposed to cytomix and DPG (300 μM) were grown at confluence on a microscope glass slide for 24 h. Then, cells were fixed in formalin 4% in PBS for 10 min. Cells were washed in PBS, permeabilized by incubation in PBS 0.1% Triton X-100 (Sigma) for 10 min and then blocked in PBS 1% BSA for 30 min. For ZO-1 (Tight junction protein-1) staining samples were incubated with anti-ZO-1 (1:100, BD Trasduction Laboratories) for 1 h and then with the secondary anti-mouse antibody AlexaFluor 488 (Molecular Probes, Eugene, OR, USA) for 30 min. F-actin was stained with Alexa Fluor 488-conjugated Phalloidin (1:50, Molecular Probes) according to manufacturer's instructions. 4′,6-diamidino-2-phenylindole (DAPI) was added for nuclei counterstaining. Quantification of ZO-1 and F-actin fluorescent signal relative to DAPI was performed using Image J software.

TABLE 1 | List of murine primers used in RealTime PCR.

Gene	Forward primer sequence 5′ → 3′	Reverse primer sequence 5′ → 3′
IL-1β	GAGGCAGTATCACTCAATG	CGTTGCTTGGTTCTCCTTGT
Il-6	CAAGTCGGAGGCTTAATTACACATG	AGAAAAGAGTTGTGCAATGGCA
CCL12	GTTGGCTCAGCCAGATGAA	AGGCTACTCATTGGGATCATCTTG
CXCL3	GAAGATTACTGAAGAGCGGCAAGTC	AATGCAGGTCCTTCATCATGGT
CXCL5	CGTAACTCCAAAAATTAATCCCAAA	CGAGTGCATTCCGCTTAGCT
CCL7	CCTGGGAAGCTGTTATCTTCAA	AGGCTTTGGAGTTGGGGTTT
CXCL1	ACCGAAGTCATACCCACACTC	CTCCGTTACTGGGGGACACC
COL3A1	GCCCACAGCCTTCTACAC	CCAGGGTCACCATTTCTC
VTN	CCCCTGAGGCCCTTTTTCATA	CAAAGCTCGGTCACACTGACA
CSF3	GTATAAAGGCCCCCTGGAGCTG	TGCAGGGCCATTAGCTTCAT3
FGF2	GGAGGGCTGCTGGCTTCTAA	CCAGTTCGTTTCAGTGCCACATAC
FGF7	GAACAAAAGTCAAGGAGCAACC	GTCATGGGCCTCCTCCTATT
MMP9	TGTCTGGAGATTCGACTTGAAGTC	TGAGTTCCAGGGCACACCA
TIMP1	CTGGCATCTGGCATCCTCTT	TAGCCCTTATGACCAGGTCCG
PLAT	AGATGAGCCAACGCAGACAA	GTTGGTTGGCTGCAACTTGC
PLAUR	GTGGCCCAGTTCTGGATCTT	GATGAGAGACGCCTCTTCGG
SERPINE1	ACTGCAAAAGGTCAGGATCG	ACAAAGGCTGTGGAGGAAGA
PTGS2	AAGTGCGATTGTACCCGGAC	GTGCACTGTGTTTGGAGTGG
TNF	CAGACCCTCACACTCAGATCATCTT	TCGTAGCAAACCACCAAGTGG
IL-10	AACAAAGGACCAGCTGGACAAC	GGCAACCCAAGTAACCCTTAAA
GAPDH	AACTTTGGCATTGTGGAAGG	CACATTGGGGGTAGGAACAC

Trans-epithelial Electrical Resistance (TEER) Measurements

Caco2 cells were seeded at a density of 1.0×10^5 cells/well on ThinCert™ Cell Culture Inserts (24 well, 0.4 μm pore size, Greiner) and were differentiated for 16 days. Cellular TEERs were measured with an electrical resistance system, EVOM2, Epithelial Volt/Ohm Meter for TEER (EVOM2-TEER, WPI). When the cells reached a stable TEER readings >2,000 øcm^2, cytomix or co-treatment with cytomix and DPG (300 μM) were supplied to apical and basal compartments of transwell chambers for 96 h. In a second set of experiments, cells were treated with cytomix for 24 h and TEER value was measured (t0); Cells were then exposed to DPG 300 μM (SIGMA), anti-VTN (1:1,000) and anti-PLAUR (1:1,000), alone or in combination for 48 h. In both case, TEER measurements were daily acquired. Results were expressed as percentage relative to the ratio between initial and TEER value at different time points.

Statistics

All statistical analyses were performed with GraphPad InStat software (GraphPad Software, San Diego, CA, USA). The Kolmogorov–Smirnov test was used to assess whether data were sampled from populations following the gaussian distribution. Comparison among groups was performed using the Kruskal-Wallis Test with Dunn's Multiple Comparisons *post-test*.

For *in vitro* studies, all experiments were repeated three times and data were given as mean ± standard deviation (SD). Comparisons among groups was performed by Mann–Whitney test. Differences were noted as significant * $p < 0.05$, ** $p < 0.01$, *** $p < 0.001$.

RESULTS

DPG Down-Regulates the Expression Levels of MH Genes Altered by Inflammation in Mice With Experimental Acute Colitis

We used an array of 84 genes of wound healing pathway to identify those more influenced by DPG in the colonic tissue of mice with acute colitis. C57BL/6 mice were randomly divided into three groups: control group received regular drinking water, mice treated with 3% DSS to induce colitis and mice treated with 3% DSS and 8 mg/kg/day DPG, daily administered by oral gavage. After 7 days, mice were sacrificed and the colon removed. RNA obtained from colon tissue of controls, DSS-induced colitis and mice co-treated with DSS and DPG, were analyzed by a PCR array. Results showed that inflammation induced by DSS caused a strong up-regulation of 24 out of 84 genes ($p < 0.05$), of which, 20 were significantly down-regulated by DPG administration (**Figure 1A**). Statistical assessment of the False Discovery Rate demonstrated that all identified modulation was significant (**Supplementary Material 1**). The 20 genes, down-regulated by DPG, were classified into the following functional groups: (1) *cytokines* (IL-10, IL-1β, IL-6, TNF); (2) *chemokines* (CCL12, CCL7, CXCL1, CXCL3, CXCL5); (3) *extracellular matrix components* (COL3A1, VTN); (4) *growth factors* (CSF3, FGF2, FGF7); (5) *extracellular matrix remodeling enzymes* (MMP9,

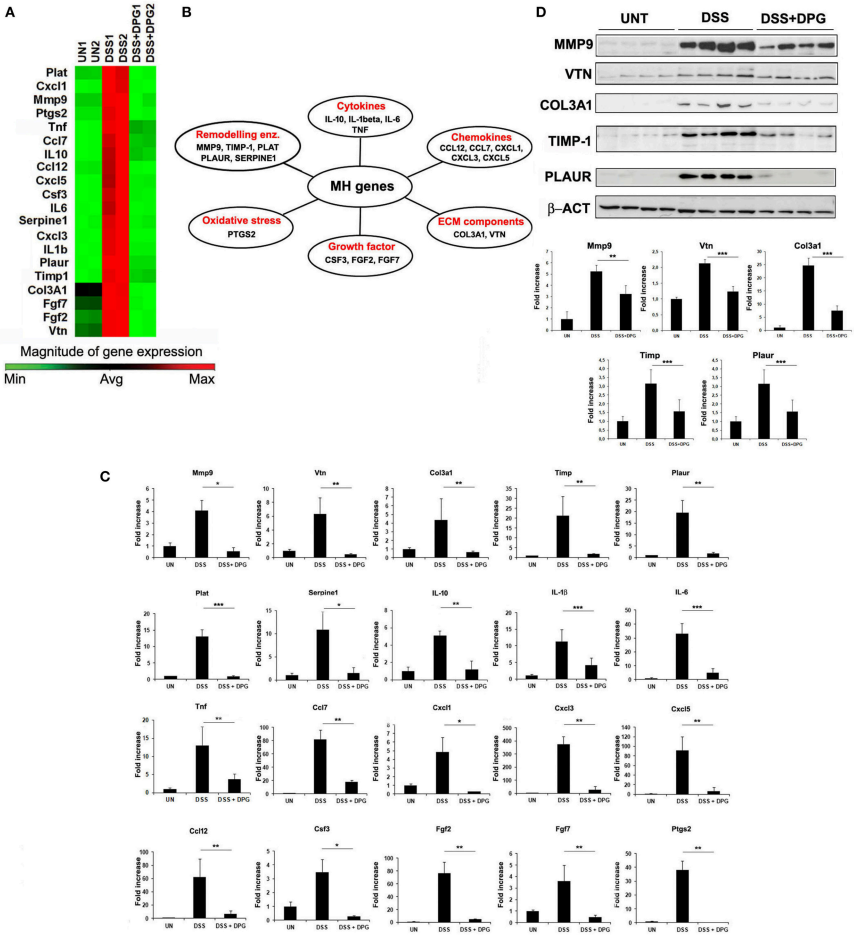

FIGURE 1 | Identification and validation of genes, involved in MH pathways, modulated by DPG in inflamed tissues of mice with experimental acute colitis. **(A)** Genes activated by DSS and inactivated by DPG treatment *in vivo*, identified by PCR-Array, and **(B)** their classification in functional groups. **(C)** mRNA expression of all identified genes, modulated by DPG in mice with DSS acute colitis, were validate by quantitative real-time PCR. Statistical analysis: Kruskal-Wallis Test with Dunn's Multiple Comparisons *post-Test*. **(D)** Protein expression of some identified genes was confirmed by western blot, using 8 animals per group. Statistical analysis: Kruskal-Wallis Test with Dunn's Multiple Comparisons *post-Test*. $^{*}p < 0.05$, $^{**}p < 0.01$, $^{***}p < 0.001$. PCR-Array was repeated in triplicate using a pool of RNA obtained from 5 animals per group. Real-time PCR values are mean ± St. dev. of 8 animals per experimental group and data represent the target gene expression normalized to the reference gene. UN, untreated animals; DSS, dextran sulfate sodium; DPG, dipotassium glycyrrhizate.

TIMP1, PLAT, PLAUR, SERPINE1); (6) *oxidative stress* (PTGS2) (**Figure 1B**). The effect of DPG on mRNA expression of this gene set was then confirmed by RealTime-PCR ($p < 0.001$: IL-1beta, IL-6, PLAT; $p < 0.01$: IL-10, TNF, CXCL3, CXCL5, CCL12, CCL7, COL3A1, VTN, FGF7, FGF2, TIMP1, PLAUR, PTGS2; $p < 0.05$: CXCL1, MMP9, SERPINE1, CSF3) (**Figure 1C**).

TABLE 2 | List of the mucosal healing pathway genes analyzed.

Gene	Fold regulation comparing DSS vs. UN	Fold regulation comparing DSS+DPG vs. DSS	
Cxcl3	1083.85	−165.97	
Il6	425.18	−102.17	
Csf3	335.14	−55.9	
Il1b	204.88	−37.48	
Il10	60.91	−9.35	
Ifng	49.13	−2.87	*Excluded DSS+DPG vs. DSS < 3.5 folds
Cxcl5	44.38	−21.33	
Cxcl1	28.68	−37.57	
Timp1	26.09	−8.5	
Ccl7	25.61	−7.15	
Tnf	17.09	−5.43	
Plaur	14.61	−8.78	
Ptgs2	13.04	−30.87	
Serpine1	10.55	−9.77	
Vtn	8.43	−40.55	
Ccl12	7.88	−10.94	
Plat	7.65	−24.16	
Mmp9	7.37	−15.05	
Hgf	7.14	−3.42	*
Fgf2	5.32	−27.25	
Fgf7	5.02	−28.67	
Fga	4.98	−2.46	*
Mmp7	4.87	−1.11	*
Col3a1	3.69	−20.75	
Tgfbr3	3.29	−8.56	From here excluded because DSS vs. UN < 3.5 folds
Cd40lg	3.28	1.65	
Mmp2	3.14	−5.55	
Tgfb1	3.12	−2.9	
Wisp1	3.1	−7.63	
Igf1	3.05	−5.33	
Il2	2.9	−4.12	
Col4a1	2.87	−9.7	
Fgf10	2.87	−16.81	
Cxcl11	2.84	−13.16	
Il4	2.77	−7	
F13a1	2.75	−6.89	
Itga4	2.55	−4.43	
Il6st	2.44	−4.13	
Itgav	2.43	−5.09	
Ctsk	2.33	−4.62	
Ctsg	2.21	−1.09	
Wnt5a	2.2	−6.11	
Plau	2.13	−4.31	
Angpt1	1.88	−3.51	
Col5a1	1.88	−5.81	
Plg	1.87	−1.14	
Col1a1	1.86	−2.32	
Itgb6	1.81	−3.41	
Stat3	1.79	−2.59	
Egfr	1.78	−4.44	
Itgb1	1.57	−4.24	
Col5a2	1.52	−9.03	
Itga5	1.52	−4.78	
Col1a2	1.44	−6.2	
Col5a3	1.39	−6.06	
Itga3	1.34	−1.48	
Itgb3	1.34	−3.19	
Itga2	1.17	−1.89	
Ctsl	1.16	−5.69	
F3	1.13	−3.34	
Itgb5	1.13	−2.25	
Hbegf	1.12	−6.42	
Mif	1.07	1.42	
Mmp1a	−1.01	−3.83	
Itga1	−1.04	−2.94	
Vegfa	−1.14	−1.39	
Ctnnb1	−1.22	−1.76	
Tagln	−1.23	−3.85	
Itga6	−1.25	−1.67	
Ctgf	−1.28	−11.17	
Rhoa	−1.29	−1.79	
Pdgfa	−1.35	−2.75	
Col14a1	−1.38	−1.9	
Pten	−1.4	−3.28	
Mapk3	−1.44	−1.06	
Mapk1	−1.44	−1.51	
Tgfa	−1.46	−1.52	
Cdh1	−1.56	−1.45	
Rac1	−1.66	−3.12	
Egf	−2.02	−2.22	
Csf2	−2.03	1.57	
Acta2	−2.13	−2.35	
Col4a3	−4.53	−1.52	
Actc1	−6.72	1.21	

Inclusion criteria for the genes were the following: fold-regulation comparing DSS vs. UN > 3.5 folds; furthermore for those included fold-regulation comparing DSS+DPG vs. DSS > 3.5.
The genes were shown in order of decreasing up-regulation comparing DSS vs. UN.
The genes positive for the inclusion criteria were highlighted in gray.
**Genes excluded because DSS+DPG vs. DSS < 3.5 folds.*

Moreover, a subset of genes (MMP9, VTN, COL3A1, TIMP1, and PLAUR), chosen among those more directly involved in the tissue remodeling process, were also analyzed by western blot. Results again showed that the expression levels of all genes previously altered by the DSS treatment was reduced by DPG (MMP9: $p < 0.01$; VTN, COL3A1, TIMP-1, PLAUR: $p < 0.001$) (**Figure 1D**). Complete list of 84 mucosal healing pathway genes analyzed

was reported in **Table 2**. Moreover, data set of the microarray carried out are available on Gene Expression Omnibus platform (GEO) with accession number GSE127953 and provided as **Supplementary Material 1**.

This result was also confirmed *in vitro* by exposing Caco2 and HT-29 cells to pro-inflammatory cytokines (cytomix: TNF-α and IFN-γ) or co-exposing to cytomix + DPG and analyzing the protein expression of MMP9, VTN, COL3A1, TIMP1, and PLAUR by western blot. Results revealed a significant increase only of VTN, TIMP1 and PLAUR expression from 6 up to 24 and 48 h ($p < 0.001$) after cytomix exposure, however, co-exposure to DPG completely reverted to normal values (VTN and TIMP-1: $p < 0.001$; PLAUR: 6 h $p < 0.001$, 24–48 h $p < 0.01$) (**Figure 2**).

Exposure to DPG Restores the Proper Structural Organization, Wound Repair Ability, and Functionality of Intestinal Epithelial Barrier Altered During Inflammation

To evaluate the effect of DPG on epithelial barrier morphology, differentiated Caco2 and HT29 cells were exposed to cytomix or co-exposed to cytomix and DPG for 24 h. Cell-cell adhesion and intestinal epithelium organization were assessed by analyzing the expression levels of zonulin-1 and the formation of stress fibers (SFs), through immunofluorescence. All cells exposed to cytomix showed a strong reduction of zonulin-1 expression, with consequent loss of tight junction (TJ) adhesion, and an evident increase of SFs leading to a loss of proper tissue architecture. However, the exposure to DPG restored the original setting (ZO-1/DAPI fluorescence: UN: 0.55 ± 0.03; cytomix: 0.27 ± 0.13; cytomix + DPG: 0.65 ± 0.05); (F-actin/DAPI fluorescence: UN: 0.31 ± 0.05; cytomix: 1.30 ± 0.14; cytomix + DPG: 0.25 ± 0.05) (**Figures 3A,B** and **Supplementary Figures 1A,B**).

Furthermore, to assess whether DPG influences intestinal cell migration, a scratch test was performed. Since DPG is an inhibitor of HMGB1 we include a treatment with HMGB1 B box (B-box), which is the recombinant truncated form of the protein consisting of the pro-inflammatory component as well a treatment with anti-HMGB1 antibody, used to block HMGB1. Hence, confluent HT29 and Caco2, exposed to cytomix or to B-box in presence or absence of DPG or anti-HMGB1 antibody, were scratched with a 10 µl micropipette tip and the gap widths (1 mm at day 0) were measured after 24 and 48 h. Wound healing was estimated after 48 h as cellular density related to a fixed wounded area (1 mm^2). Results showed that the cytomix exposure caused a delay in healing as compared to untreated cells (cellular density: cytomix 16.63 ± 0.95; UN 187.84 ± 8.25), however, co-treatment with DPG or with anti-HMGB1 antibody strongly reduced the delay, showing a complete repair after 48 h (cellular density: cytomix + DPG 171.15 ± 9.30; cytomix + anti-HMGB1 antibody 167.72 ± 17.78). Besides also B-box exposure caused a delay in healing strongly reduced by DPG (cellular density: B-box 26.39 ± 7.22; B-box + DPG 131.89 ± 11.53) (**Figure 3C** and **Supplementary Figure 1C**). Finally, the functionality of intestinal epithelial barrier was analyzed through the trans epithelial electrical resistance (TEER), a widely

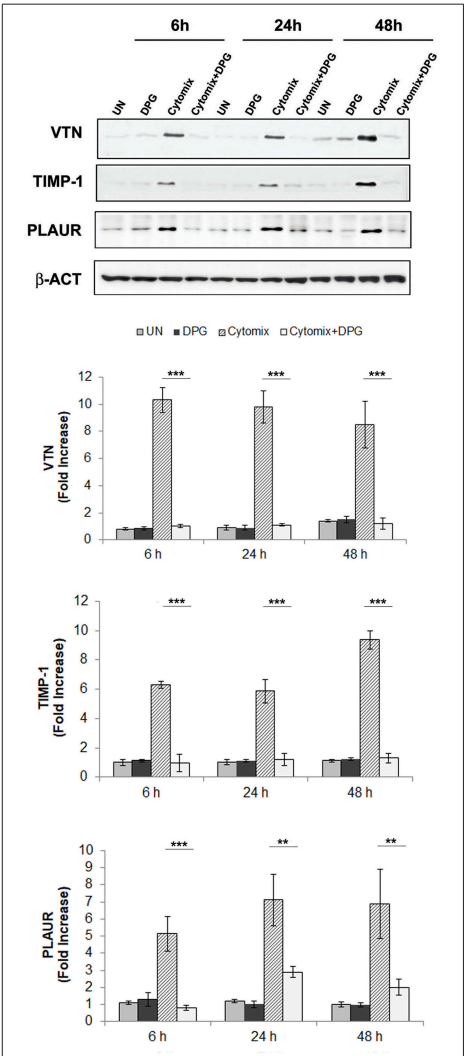

FIGURE 2 | DPG reduced *in vitro* the expression of wound healing genes: VTN, TIMP-1, and PLAUR altered by inflammatory stimulus. HT-29 cells were exposed to cytomix or co-exposing to cytomix + DPG and protein expression of VTN, TIMP1, and PLAUR were analyzed by western blot. Bar chart represented fold increase (Densitometric Unit) vs. UN. The experiment was performed in triplicate and repeated 3 times. Statistical analysis: Mann-Whitney test, the comparison between Cytomix vs. Cytomix + DPG was reported. $^{**}p < 0.01$, $^{***}p < 0.001$. UN, untreated cells; DPG, dipotassium glycyrrhizate.

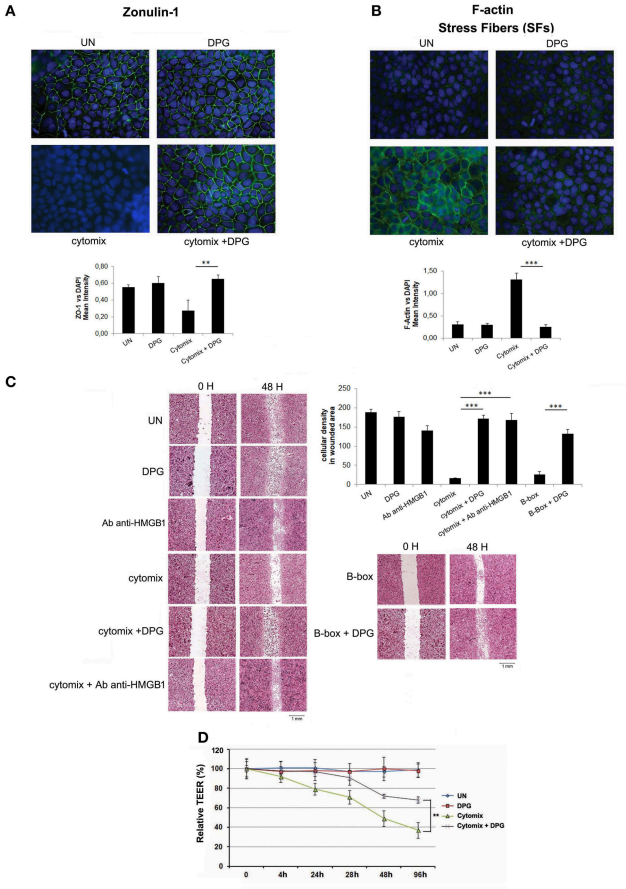

FIGURE 3 | DPG improves *in vitro* epithelial barrier functions and morphology. Zonulin-1 and F-actin expression and localization were determined by immunofluorescence in Caco2 treated with Cytomix, DPG and Cytomix + DPG Results are presented as Mean intensity of ZO-1 and F-actin fluorescence, relative to DAPI ± S.D, respectively. Magnification 20X **(A,B)** Scratch test and bar chart of cellular density of wounded area in HT29 **(C)** and TEER values **(D)** indicated wound healing in Caco2 cells treated with Cytomix, DPG, and Cytomix + DPG. The experiment was performed in triplicate and repeated 3 times. Statistical analysis: Mann-Whitney test.** $p < 0.01$, *** $p < 0.001$. UN, untreated cells; DPG, dipotassium glycyrrhizate.

accepted quantitative technique to measure the integrity of tight junction (TJ) dynamics. TEER was applied to Caco2 cells that, when cultured until confluence, become a monolayer and differentiate spontaneously to enterocytes developing TJ on the apical side and getting excellent barrier functions (2 weeks culturing). After differentiation, cytomix or DPG+cytomix were given to the apical side of Caco2. Results showed that TEER values were significantly decreased in cells exposed to cytomix compared to physiological condition, indicating a loss of barrier functions (TEER value: 40% vs., untreated cells (TEER value: 100%) after 96 h of culture), while, DPG addition caused a sharp increase of TEER values, indicating a reliable recovery of barrier functions (TEER value: 70% after 96 h of culture) (**Figure 3D**).

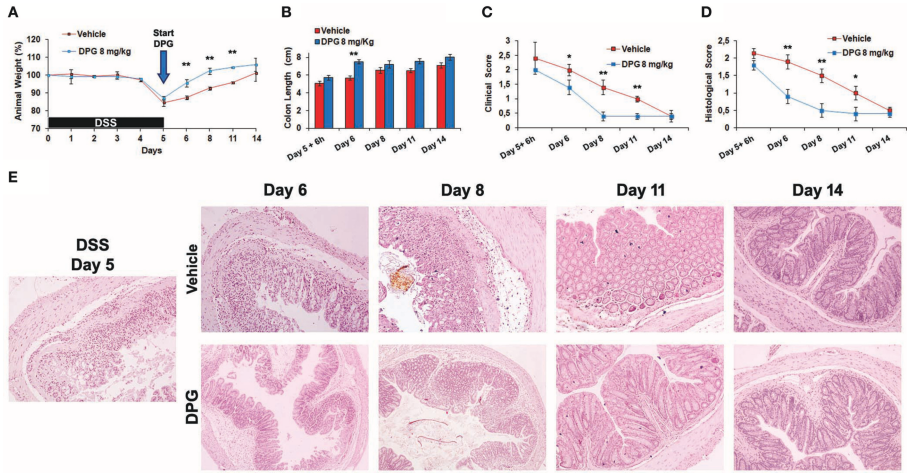

FIGURE 4 | DPG accelerates mucosal healing during recovery phase of DSS-induced acute colitis. C57BL/6 mice were treated with 3% DSS for 5 days and then were untreated or treated with DPG (8 mg/kg) for successive 9 days. Following parameters were analyzed: **(A)** weight loss; **(B)** colon length; **(C)** clinical score (stool consistency, presence of blood in stool and general appearance); **(D)** histological score; **(E)** morphology of the colon evaluated through histological analysis (40x magnification in the image). Five animals per experimental group were used. Statistical analysis: Kruskal-Wallis Test with Dunn's Multiple Comparisons *post-Test*. $^{*}p < 0.05$, $^{**}p < 0.01$. UN, untreated animals; DSS, dextran sulfate sodium; DPG, dipotassium glycyrrhizate.

DPG Accelerates MH During the Recovery Phase Following the DSS-Induced Colitis in Mice by Differently Regulating Pro-inflammatory and Wound Healing Genes

To investigate the effects of DPG on MH during the recovery phase following the induction of acute colitis, a time-course experiment was set up: mice were treated with DSS for 5 days and then with DPG (or a vehicle as placebo) for following 6-24-72-144-216 h (recovery time). Firstly, weight, colon length, clinical score and histological score were assessed. Results showed that mice treated with DPG had a faster recovery already visible at 24 h (day 6). Full recovery was obtained at 72 h (day 8) in DPG-treated mice and at 144 h (day 11) in vehicle-treated mice. In particular, at 24 h, DPG-treated mice recovered weight: 95 ± 2 vs. 87 ± 1.1% of vehicle-treated mice ($p < 0.01$) (**Figure 4A**); colon length: 7.5 ± 0.43 cm vs. 5.7 ± 0.33 cm of vehicle ($p < 0.01$) (**Figure 4B**); clinical score: 2.0 ± 0.2 vs. 1.4 ± 0.25 of vehicle ($p \leq 0.05$) (**Figure 4C**); histological score: 0.9 ± 0.2 vs. 1.9 ± 0.3 of vehicle ($p < 0.01$) (**Figures 4D,E**).

Furthermore, since results above show that the highest recovery rate occurred in the time window between 6 and 72 h (following the interruption of DSS), the mRNA levels of previously identified 19 genes were also analyzed in this time lapse. Results showed, post-DSS treatment, an increase of inflammatory molecules CXCL1, CXCL3, CXCL5, PTGS2, IL-1β, IL-6, CCL12, and CCL7 that were significantly reduced (24 h: $p < 0.001$: CXCL1, CXCL3; $p < 0.01$: PTGS2, IL-1β, IL-6; $p < 0.05$: CXCL5, CCL7, CCL12, IL-10) within the 72 h (back to control values) by DPG treatment (**Figure 5A**). Interestingly, DPG induced a significant increase (24 h: $p < 0.001$: MMP9, PLAUR, FGF2; $p < 0.01$: COL3A1, VTN, SERPINE, CSF3, FGF7; $p < 0.05$: TIMP1) of genes more directly involved in the wound healing, such as COL3A1, MMP9, VTN, PLAUR, SERPINE, CSF3, FGF2, FGF7, PLAT, and TIMP1, at earlier time (between 6 and 24 h) (**Figure 5B**). Noticeably, this result is not observed in untreated mice. Among all, the two most up-regulated genes by DPG, VTN and PLAUR, were also analyzed by western blot. Results confirmed that protein expression of both genes was significantly increased by DPG (VTN: 24–72 h $p < 0.01$; PLAUR: 6–24 h $p < 0.01$, 72 h $p < 0.01$) between 6 and 72 h comparing to untreated mice, but expression came back to control values at the end of treatment (day 14) (**Figure 5C**).

The ECM Remodeling Proteins PLAUR and VTN Are Crucial to Achieve MH During DPG Treatment

To investigate *in vitro* the role in MH of PLAUR, the most DPG-activated gene during the recovery phase from colitis at 6 h, as

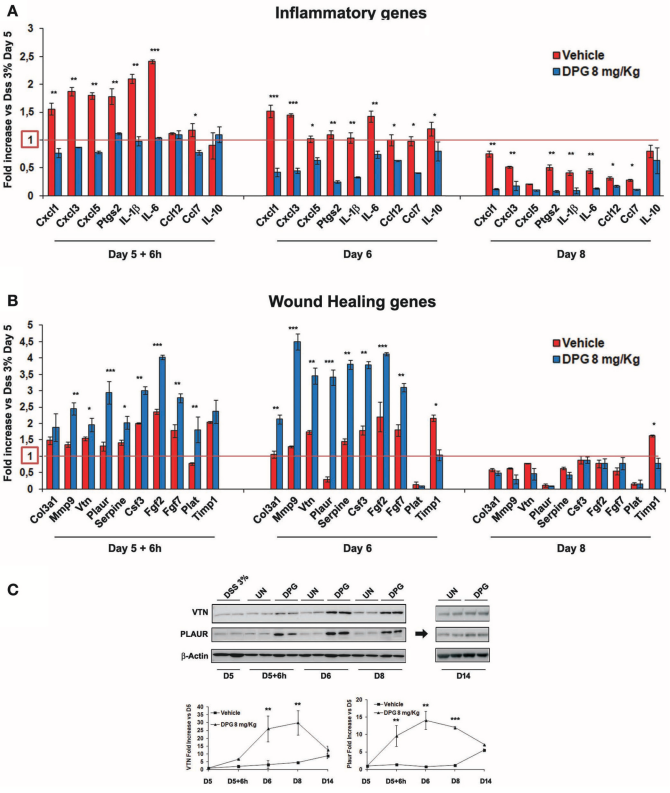

FIGURE 5 | DPG improves mucosal healing *in vivo* by reducing pro-inflammatory genes and increasing wound healing genes. C57BL/6 mice were treated with DSS for 5 days and then were untreated or treated with DPG (8 mg/kg) for successive 9 days. During remission phase, gene expression of all **(A)** pro-inflammatory and **(B)** wound healing genes, previously identified, was analyzed by real-time PCR at the following time point: 5th day+6h, 6th day, and 8th day. Real-time PCR values are mean +/– St. dev. of 5 animals per experimental group and data represent the target gene expression normalized to the reference gene. The expression level after 5 days of DSS treatment was taken as 1 for each gene. **(C)** VTN and PLAUR were also analyzed by western blot**.** Upper panel: western blot; bottom panel: fold increase vs. day 5th calculated using optical densitometry. Five animals per experimental group were used. Statistical analysis: Kruskal-Wallis Test with Dunn's Multiple Comparisons *post-Test.**$p < 0.05$, **$p < 0.01$, ***$p < 0.001$. UN, untreated animals; DSS, dextran sulfate sodium; DPG, dipotassium glycyrrhizate.

well as its ligand VTN, we observed the ability to repair and barrier function recovery of intestinal epithelial cells, exposed in time order to cytomix and DPG, in which VTN and PLAUR were alternately inhibited by specific antibody. Hence, Caco2 and HT29 cells were exposed to the cytomix for 24 h and then exposed to DPG for the following 6, 24, and 48 h. Firstly, results revealed that PLAUR and VTN expression significantly increased ($p < 0.001$) at 6 h following DPG and came back to normal values from 24 to 48 h (**Figure 6A**). Since this effect could indicate that these genes were required for an efficient MH, we carried out a scratch test and a TEER assay in inflamed epithelial cells in which VTN or PLAUR were inhibited by specific antibody. Thus, Caco2, and HT29 cells were treated with cytomix for 24 h, then cytomix was removed and DPG or DPG+antibody anti-VTN or DPG+antibody anti- PLAUR were added for the following 48 h for scratch test and up to 72 h for TEER assay. Results showed that the increase of TEER and wound closure rates induced by DPG was reverted by inhibition of VTN or PLAUR, suggesting that both genes are crucial in achieving MH during DPG treatment (**Figures 6B,C**).

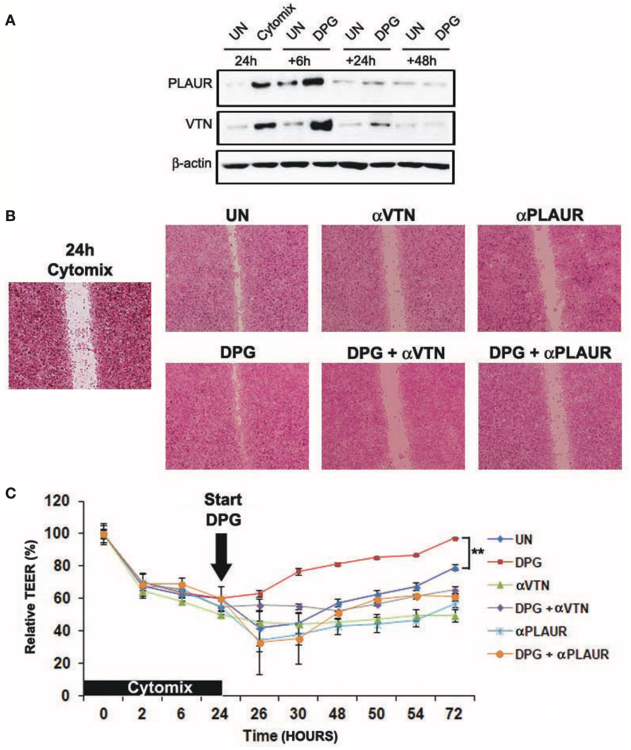

FIGURE 6 | Proteins VTN and PLAUR are fundamental to achieve mucosal healing during DPG treatment *in vitro*. HT29 cells were pre-treated with cytomix for 24 h and then were exposed to DPG for 6, 24, and 48 h. **(A)** VTN and PLAUR expression was analyzed by western blot. In the same experimental condition as above HT29 or Caco2 were treated with DPG, with an anti-Plaur antibody or with the inhibitor of VTN, alone or in combination with DPG and **(B)** wound healing and **(C)** epithelial barrier integrity were evaluated by scratch test (HT29) and TEER (Caco2), respectively. The experiments were repeated in triplicate. Statistical analysis: Mann- Whitney test $^{**}p < 0.01$. UN, untreated cells; DPG, dipotassium glycyrrhizate.

DISCUSSION

Gut MH is a complex and dynamic process of replacing devitalized and missing cellular structures and tissue layers involving the coordinated activity of intestinal epithelial cells (20, 21). The ability of factors in modulating MH proteins and enhance intestinal repair mechanisms may form the basis of future approaches for treating diseases characterized by epithelial surface damage (22), since MH is emerging as a critical endpoint in clinical trials and practice (4). Indeed, it was shown that IBD patients who achieve and maintain MH have more favorable long-term outcomes compared to patients who do not get it (5). In the past two decades, anti-TNFα therapy was found to induce endoscopic remission and sustained mucosal healing (23), however, many patients (∼40%) do not respond, lose their response during treatment, or develop complications due to side effects (24, 25). Recently, additional therapies were aimed to improve MH, such as vedolizumab (integrin blocker) and ustekinumab (anti-p40 subunit of IL-12/IL-23), mainly in patients unresponsive to anti-TNFα, but beneficial results are still variable and side effects persist (19, 26, 27).

In a previous study, the DPG was shown to importantly reduce the DSS-induced colitis in mice without collateral effects (17). In the present study, we firstly aimed to assess *in vivo* the ability of DPG to modulate a panel of MH genes. Accordingly, we induced the experimental acute colitis in mice and observed that DPG strongly down-regulated to control values 20 genes involved in different MH pathways (mainly represented by cytokine,

chemokine and ECM genes), altered by inflammation. To deeply explore *in vitro* the effects of DPG on the gut barrier during the acute phase of inflammation, intestinal epithelial cells were co-exposed to inflammatory agents and DPG. Structural integrity of the intestinal epithelium was investigated by analyzing the modulated expression of the adhesion molecule, zonulin-1, and the dynamic alteration in actin fiber development. We found that DPG noticeably improved the expression levels of zonulin-1, strongly decreased by inflammation, and reduced the number of F-actin stress fibers resulting in response to inflammatory stimuli, altering the cell cytoskeleton organization. Moreover, since epithelial cell migration during healing represents an important mechanism to rescue the tissue integrity, we also looked at wound closure ability of intestinal cells and found that DPG significantly accelerated the healing rate during inflammation, improving epithelial barrier integrity but also its proper functioning, as seen by TEER assay. Of interest, rescue in tissue integrity due to DPG was observed when inflammation was trigger both by cytomix or B-box, suggesting that this effect is mediated by HMGB1 inhibition.

All these findings highlight the efficacy of DPG on improving wound healing during acute inflammation and, consequently, promoting the mucosal integrity, that is essential to preserve the epithelial functions. Indeed, patients with different gastrointestinal disorders, such as IBD, acute gastritis or pancreatitis, and celiac disease, are all phenotypically characterized by severely compromised epithelial barriers (22, 28) and re-establishment of barrier integrity is often associated with clinical remission and improved outcome (29).

In our study we found that the, DPG, an HMGB1 inhibitor, promote healing. Recently Tirone et al. (30), showed that HMGB1 promotes healing. Although these studies seem to disagree each other, the differences could be explained by the HMGB1 redox state. Indeed literature data reported that fully reduced HMGB1 (fr-HMGB1) acts as a chemo attractant for cells (31), whereas HMGB1 containing a disulfide bond (ds-HMGB1) is a pro-inflammatory molecule (32); further cysteine oxidation to sulfonates by reactive oxygen species abrogates both activities (33). To dissect the various activities of HMGB1, Tirone et al. created a mutant (3S) in which the cysteines are replaced with serines, which are resistant to sequential oxidation. Collectively, their results revealed that, after acute injury, muscle and liver regeneration were specifically promote by fr-HMGB1 and 3S. Furthermore, HMGB1 activities was analyzed during sterile injury. In our study we tested the effect of DPG, an HMGB1 inhibitor, on healing promotion in an inflammatory context. Probably, in our condition the prevalent form of HMGB1 should be the ds-HMGB1, with cytokine-inducing activity, and the DPG inhibiting it promotes healing.

Besides, we were interested to assess the effects of DPG during the recovery phase from colitis, as well. Thus, in a second set of experiments, mice were exposed to DSS and then let untreated (controls) or were treated with DPG for following 6, 24, 72, 144, or 216 h (recovery time). Intriguingly, we found that DPG-treated mice showed an evident improvement of body weight, colon length, clinical, and histological score as compared to controls. More interestingly, we observed since the earliest time (6 h) an opposite effect of DPG on MH gene expression: a significantly decrease of inflammatory genes (CXCL1, CXCL3, CXCL5, PTGS2, IL-1β, IL-6, CCL12, CCL7) and a simultaneous increase of ECM components/remodeling enzymes (COL3A1, MMP9, VTN, PLAUR, SERPINE, CSF3, FGF2, FGF7, PLAT, and TIMP1). These results clearly suggest that, within a narrow time window (between 6 and 24 h from the ending of DSS and the beginning of DPG treatment), while DPG is reducing inflammation, concurrently, is prompting the tissue rescue by implementing ECM remodeling genes. When inflammation is dampened (72 h following DPG treatment), ECM remodeling genes as well as inflammatory genes were wholly down-regulated. It is worth noting that it was possible to highlight the dual achievement of DPG only setting up a recovery phase experiment, indeed, we did not have this evidence in mice with the acute colitis.

These data drawn our attention on the role of ECM in MH. ECM is a highly dynamic structure present in all tissues continuously undergoing controlled remodeling that is critical for regulating the morphogenesis of different organs, including the intestine. Interestingly, ECM is established to be integral to wound healing, with a close relationship occurring between ECM deregulation and altered healing. In order to understand whether the ECM remodeling enzyme PLAUR, the most activated gene by DPG during the earlier recovery phase from colitis, as well as its ligand VTN, were critical for DPG-induced MH, we exposed to cytomix followed by DPG the intestinal cells, in which the two genes were alternately inhibited by specific antibodies. PLAUR, also known as urokinase-type plasminogen activator receptor (uPAR) is a part of the plasminogen activation system and is activated by several ligands as Serine protease urokinase-type plasminogen activator (uPA), VITRONECTIN (34) and inhibited by SERPINE1 (35).

Results showed that wound healing ability as well as epithelial barrier functions were importantly impaired by inhibition of both genes in inflamed cells then exposed to DPG. This evidence strongly suggests that VTN and PLAUR expression is mandatory to promote tissue repair even in cells in which MH is improved by DPG treatment. It is worth noting that under physiological conditions, PLAUR is thought to have fairly limited tissue expression. This receptor is expressed during ECM remodeling, for example in gestational tissues during embryo implantation and placental development (36) and in keratinocytes during epidermal wound healing (37). Stress, injury and inflammation also induce PLAUR expression. PLAUR-deficient mice exhibit pathological abnormalities related to PLAUR proteolytic function, including dermal fibrosis (38) and exacerbation of experimentally induced kidney fibrosis and nephropathy (39).

In conclusion, this study shows for the first time that: (1) DPG is able to modulate *in vivo* MH genes and restore *in vitro* the proper structural organization, wound repair ability and functionality of intestinal epithelial barrier during acute inflammation; (2) DPG increases ECM remodeling gene expression during the earlier recovery phase following the induction of colitis in mice; (3) the ECM genes, PLAUR and VTN, are pivotal to get MH in cells treated with DPG.

We are suggesting that the use of DPG would represent in the future an innovative and powerful tool for the treatment of human inflammatory complex disorders, including IBD.

ETHICS STATEMENT

Experimental procedures were previously approved by the Ministry of Health and the study was carried out in accordance with the Italian regulations on animal welfare. The protocol was approved by the Committee on the Ethics of Animal Experiments of the Italian National Agency for New Technology, Energy and Sustainable Economic Development (ENEA-Permit Number: 1175/2016-PR).

AUTHOR CONTRIBUTIONS

LS and RV conceived and designed experiments. LS, FP, and ABM performed experiments and analyzed data. AN contributed to data analysis. EC and VC supervised *in vitro* analysis. SC and SI supervised the work. LS and RV wrote the manuscript.

FUNDING

This work was supported by Accademic Funding of Sapienza University of Rome.

SUPPLEMENTARY MATERIAL

The Supplementary Material for this article can be found online at: https://www.frontiersin.org/articles/10.3389/fimmu.2019.00939/full#supplementary-material

Supplementary Material 1 | Complete data set and False Discovery Rate of the microarray performed.

Supplementary Figure 1 | DPG improves *in vitro* epithelial barrier functions and morphology. Zonulin-1 and F-actin expression and localization were determined by immunofluorescence in HT29. Treatment with DPG increases expression of **(A)** Zonulin-1 and reduces level of **(B)** F-actin altered by Cytomix. DPG significantly improved **(C)** wound healing in Caco2 cells, inhibited by Cytomix. UN, untreated cells; DPG, dipotassium glycyrrhizate.

REFERENCES

1. Coleman OI, Haller D. Bacterial signaling at the intestinal epithelial interface in inflammation and cancer. *Front Immunol.* (2018) 8:1927. doi: 10.3389/fimmu.2017.01927
2. Stidham RW, Higgins PDR. Colorectal cancer in inflammatory bowel disease. *Clin Colon Rectal Surg.* (2018) 31:168–78. doi: 10.1055/s-0037-1602237
3. Atreya R, Neurath M. Current and future targets for mucosal healing in inflammatory bowel disease. *Visc Med.* (2017) 33:82–8. doi: 10.1159/000458006
4. Neurath MF. New targets for mucosal healing and therapy in inflammatory bowel diseases. *Mucosal Immunol.* (2014) 7:6–19. doi: 10.1038/mi.2013.73
5. Pineton de Chambrun G, Peyrin-Biroulet L, Lémann M, Colombel JF. Clinical implications of mucosal healing for the management of IBD. *Nat Rev Gastroenterol Hepatol.* (2010) 7:15–29. doi: 10.1038/nrgastro.2009.203
6. Wu R, Dong W, Wang Z, Jacob A, Cui T, Wang P. Enhancing apoptotic cell clearance mitigates bacterial translocation and promotes tissue repair after gut ischemia-reperfusion injury. *Int J Mol Med.* (2012) 30:593–8. doi: 10.3892/ijmm.2012.1044
7. Vongsa R, Zimmerman NP, Dwinell MB. CCR6 regulation of the actin cytoskeleton orchestrates human beta defensin-2- and CCL20-mediated restitution of colonic epithelial cells. *J Biol Chem.* (2009) 284:10034–45. doi: 10.1074/jbc.M805289200
8. Neurath MF, Travis SP. Mucosal healing in inflammatory bowel diseases: a systematic review. *Gut.* (2012) 61:1619–35. doi: 10.1136/gutjnl-2012-302830
9. Andersson U, Yang H, Harris H. High-mobility group box 1 protein (HMGB1) operates as an alarmin outside as well as inside cells. *Semin Immunol.* (2018) 38:40–8. doi: 10.1016/j.smim.2018.02.011
10. Bianchi ME, Crippa MP, Manfredi AA, Mezzapelle R, Rovere Querini P, Venereau E. High mobility group box 1 protein orchestrate responses to tissue damage via inflammation, innate and adaptive immunity, and tissue repair. *Immunol Rev.* (2017) 280:74–82. doi: 10.1111/imr.12601
11. Zhu B, Zhu Q, Li N, Wu T, Liu S. Association of serum/plasma high mobility group box 1 with autoimmune diseases: a systematic review and meta-analysis. *Medicine.* (2018) 97:e11531. doi: 10.1097/MD.0000000000011531
12. Rider P, Voronov E, Dinarello CA, Apte RN, Cohen I. Alarmins: feel the stress. *J Immunol.* (2017) 198:1395–402. doi: 10.4049/jimmunol.1601342
13. Venereau E, De Leo F, Mezzapelle R, Careccia G, Musco G, Bianchi ME. HMGB1 as biomarker and drug target. *Pharmacol Res.* (2016) 111:534–44. doi: 10.1016/j.phrs.2016.06.031
14. Vitali R, Stronati L, Negroni A, Di Nardo G, Pierdomenico M, Del Giudice E, et al. Fecal HMGB1 is a novel marker of intestinal mucosal inflammation in pediatric inflammatory bowel disease. *Am J Gastroenterol.* (2011) 106:2029–40. doi: 10.1038/ajg.2011.231
15. Palone F, Vitali R, Cucchiara S, Pierdomenico M, Negroni A, Aloi M, et al. Role of HMGB1 as a suitable biomarker of subclinical intestinal inflammation and mucosal healing in patients with inflammatory bowel disease. *Inflamm Bowel Dis.* (2014) 20:1448–57. doi: 10.1097/MIB.0000000000000113
16. Palone F, Vitali R, Cucchiara S, Mennini M, Armuzzi A, Pugliese D, et al. Fecal HMGB1 Reveals microscopic inflammation in adult and pediatric patients with inflammatory bowel disease in clinical and endoscopic remission. *Inflamm Bowel Dis.* (2016) 22:2886–93. doi: 10.1097/MIB.0000000000000938
17. Vitali R, Palone F, Cucchiara S, Negroni A, Cavone L, Costanzo M, et al. Dipotassium glycyrrhizate inhibits HMGB1-dependent inflammation and ameliorates colitis in mice. *PLoS ONE.* (2013) 8:e66527. doi: 10.1371/journal.pone.0066527
18. Maxwell JR, Brown WA, Smith CL, Byrne FR, Viney JL. Methods of inducing inflammatory bowel disease in mice. current protocol in pharmacology. (2009) chapter 5: Unit 5.58. doi: 10.1002/0471141755.ph0558s47
19. Hindryckx P, Vande Casteele N, Novak G, Khanna R, D'Haens G, Sandborn WJ, et al. The expanding therapeutic armamentarium for inflammatory bowel disease: how to choose the right drug[s] for our patients? *J Crohns Colitis.* (2018) 12:105–19. doi: 10.1093/ecco-jcc/jjx117
20. Krishnan K, Arnone B, Buchman A. Intestinal growth factors: potential use in the treatment of inflammatory bowel disease and their role in mucosal healing. *Inflamm Bowel Dis.* (2011) 17:410–22. doi: 10.1002/ibd.21316
21. Sturm A, Dignass A. Epithelial restitution and wound healing in inflammatory bowel disease. *World J Gastroenterol.* (2008) 14:348–53. doi: 10.3748/wjg.14.348
22. Dignass AU. Mechanisms and modulation of intestinal epithelial repair. *Inflamm Bowel Dis.* (2001) 7:68–72. doi: 10.1097/00054725-200102000-00014
23. Rutgeerts P, Van Assche G, Sandborn WJ, Wolf DC, Geboes K, Colombel JF, et al. Adalimumab induces and maintains mucosal healing in patients with Crohn's disease: data from the EXTEND trial. *Gastroenterology.* (2012) 142:1102–11. doi: 10.1053/j.gastro.2012.01.035

24. Nielsen OH, Ainsworth MA. Tumor necrosis factor inhibitors for inflammatory bowel disease. *N Engl J Med*. (2013) 369:754–62. doi: 10.1056/NEJMct1209614
25. Leal RF, Planell N, Kajekar R, Lozano JJ, Ordás I, Dotti I, et al. Identification of inflammatory mediators in patients with Crohn's disease unresponsive to anti-TNFalpha therapy. *Gut*. (2015) 64:233–42. doi: 10.1136/gutjnl-2013-306518
26. Schreiber S, Dignass A, Peyrin-Biroulet L, Hather G, Demuth D, Mosli M, et al. Systematic review with meta-analysis: real-world effectiveness and safety vedolizumab patients with inflammatory bowel disease. *J Gastroenterol*. (2018) 53:1048–64. doi: 10.1007/s00535-018-1480-0
27. Rutgeerts P, Gasink C, Chan D, Lang Y, Pollack P, Colombel JF, et al. Efficacy of Ustekinumab in inducing endoscopic healing in patients with Chron's disease. *Gastroenterology*. (2018) 155:1045–58. doi: 10.1053/j.gastro.2018.06.035
28. Sumagin R, Parkos CA. Epithelial adhesion molecules and the regulation of intestinal homeostasis during neutrophil transepithelial migration. *Tissue Barriers*. (2015) 3:e969100. doi: 10.4161/21688362.2014.969100
29. Watson AJ, Hughes KR. TNF-α-induced intestinal epithelial cell shedding: implications for intestinal barrier function. *Ann N Y Acad Sci*. (2012) 1258:1–8. doi: 10.1111/j.1749-6632.2012.06523.x
30. Tirone M, Tran NL, Ceriotti C, Gorzanelli A, Canepari M, Bottinelli R, et al. High mobility group box 1 orchestrates tissue regeneration via CXCR4. *J Exp Med*. (2018) 215:303–18. doi: 10.1084/jem.20160217
31. Schiraldi MA, Raucci LM, Mu-oz E, Livoti B, Celona E, et al. HMGB1 promotes recruitment of inflammatory cells to damaged tissues by forming a complex with CXCL12 and signaling via CXCR4. *J Exp Med*. (2012) 209:551–63. doi: 10.1084/jem.20111739
32. Yang HP, Lundbäck L, Ottosson H, Erlandsson-Harris E, Venereau M, Bianchi E, et al. Redox modification of cysteine residues regulates the cytokine activity of high mobility group box-1 (HMGB1). *Mol Med*. (2012) 18:250–9. doi: 10.2119/molmed.2011.00389
33. Venereau E, Casalgrandi M, Schiraldi, M, Antoine DJ, Cattaneo A, De Marchis F, et al. Mutually exclusive redox forms of HMGB1 promote cell recruitment or proinflammatory cytokine release. *J Exp Med*. (2012) 209:1519–28. doi: 10.1084/jem.20120189
34. Madsen CD, Ferraris GM, Andolfo A, Cunningham O, Sidenius N. uPAR-induced cell adhesion and migration: vitronectin provides the key. *J Cell Biol*. (2007) 177:927–39. doi: 10.1083/jcb.200612058
35. Mazar AP. Urokinase plasminogen activator receptor choreographs multiple ligand interactions: implications for tumor progression and therapy. *Clin Cancer Res*. (2008) 14:5649–55. doi: 10.1158/1078-0432.CCR-07-4863
36. Uszynski M, Perlik M, Uszynski W, Zekanowska E. Urokinase plasminogen activator (uPA) and its receptor (uPAR) in gestational tissues: measurements and clinical implications. *Eur J Obste Gynecol Reprod Biol*. (2004) 114:54–8. doi: 10.1016/j.ejogrb.2003.12.006
37. Solberg H, Ploug M, Hoyer-Hansen G, Nielsen BS, Lund LR. The murine receptor for urokinase-type plasminogen activator is primarily expressed in tissues actively undergoing remodeling. *J Histochem Cytochem*. (2001) 49:237–46. doi: 10.1177/002215540104900211
38. Kanno Y, Kaneiwa A, Minamida M, Kanno M, Tomogane K, Takeuchi K, et al. The absence of uPAR is associated with the progression of dermal fibrosis. *J Invest Dermatol*. (2008) 128:2792–7. doi: 10.1038/jid.2008.157
39. Zhang G, Kim H, Cai X, López-Guisa JM, Alpers CE, Liu Y, et al. Urokinase receptor deficiency accelerates renal fibrosis in obstructive nephropathy. *J Am Soc Nephrol*. (2003) 14:1254–71. doi: 10.1097/01.ASN.0000064292.37793.FB

Conflict of Interest Statement: The authors declare that the research was conducted in the absence of any commercial or financial relationships that could be construed as a potential conflict of interest.

2. INTRODUCTION

2.1 Inflammatory bowel disease

It is widely acknowledged that IBD is an extremely complicated disease with an unclear pathogenesis. Crohn's disease (CD) and ulcerative colitis (UC) are the most common subtypes of IBD. It predominantly affects the gastrointestinal tract (GI), and results in repeated abdominal pain, diarrhea, bloody purulent stool, and weight loss, which substantially reduces the quality of life and increases the economic burden of IBD patients[1].

Characterized by chronic inflammation and inappropriate immune responses, IBD may develop into stricturing disease, penetrating disease or even colorectal cancer (CRC), posing a serious management challenge. Despite many years of research, the exact pathogenesis has not been completely elucidated. Current data indicate that IBD could be accounted as the result of the complex interplay between genetic predispositions, environmental factors, microbiota and aberrant immune responses[2].

Although recent technological advances have enormously facilitated the genetic research in IBD, the identified genetic factors can only explain a small proportion of overall disease variance[3].

Moreover, the great differences in disease manifestations between young and older patients cannot be explained merely by different genotypes; environmental factors should also be given importance due to the finding that environmental changes could shape pathological gene expression through epigenetic mechanisms[4].

Besides, the rapidly growing incidence and steadily increasing prevalence of IBD (Figure 1) further impelled us to uncover the role of the genome-environment interaction in the occurrence and development of IBD[5].

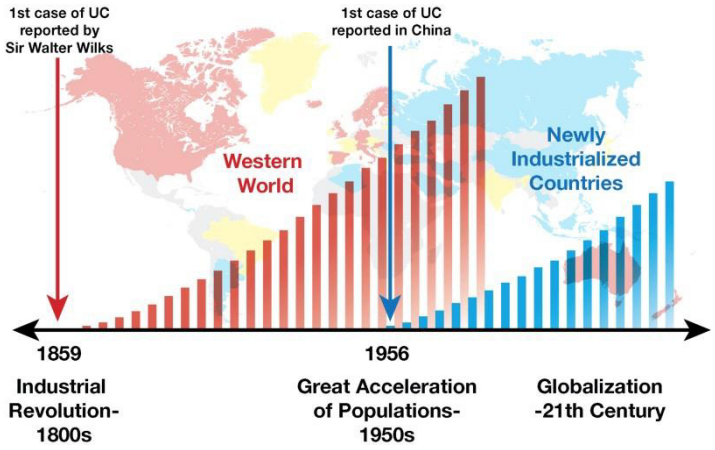

Figure 1. Increasing trend of IBD in industrialized countries since the 19th century and in industrializing countries since the 20th century. From: Keplan GG & Ng SC, Understanding and Preventing the Global Increase of Inflammatory Bowel Disease. Gastroenterology. (2017)[5].

Epigenetic mechanisms such as DNA methylation, non-coding RNAs, histone modification, and the positioning of nucleosomes significantly contribute to the interplay between genome and environment[6].

2.1.1 Clinical manifestation, diagnosis and therapy

Clinical manifestation for both CD and UC can be highly variable with enormous diversity in disease phenotypes. However, CD is characterized by transmural inflammation that can involve any part of the gastrointestinal tract, while UC typically involves superficial inflammation of the colon and rectum with extension into adjacent mucosa. CD and UC commonly present with abdominal pain, diarrhea, anaemia and weight loss. Rectal bleeding occurs more frequently in UC (83–95%) compared to CD (40%)[7].

The diagnosis of IBD requires a combination of clinical features, biomarkers, radiology, endoscopy and histopathology investigation[8].

Currently, there is no known cure for these disorders, that are therapeutically approached by four major classes of drugs: aminosalicylates, anti-inflammatory steroids, immunomodulators or biological drugs[9]. Symptoms can also be managed through diet[10]. Surgery is still required in all those cases that fail to respond to medical treatments or develop

severe complications. Currently the achieving of complete endoscopic remission, defined by the complete endoscopic healing of inflammatory lesions, is considered the goal standard in IBD treatments[11].

2.1.2 Pathogenesis

The pathogenesis of IBD is intricate and has yet to be fully understood. A complex interaction between genetic, immunological, microbial and environmental factors may explain the increasing incidence of IBD around the world (Figure 2).

Following the introduction of genome-wide association studies, the number of significant genetic risk loci in IBD has expanded progressively and novel therapeutic targets have been discovered through functional mapping of candidate gene regions. However, these risk alleles explain less than 30% of the susceptibility to disease development, suggesting that environmental factors, including the gut luminal environment, contribute considerably. The increasing occurrence of IBD in Eastern countries following their 'westernization', as well as the increased risk of disease among those who migrate to high-incidence regions, also suggest that the environment is key in the pathogenesis of IBD[12].

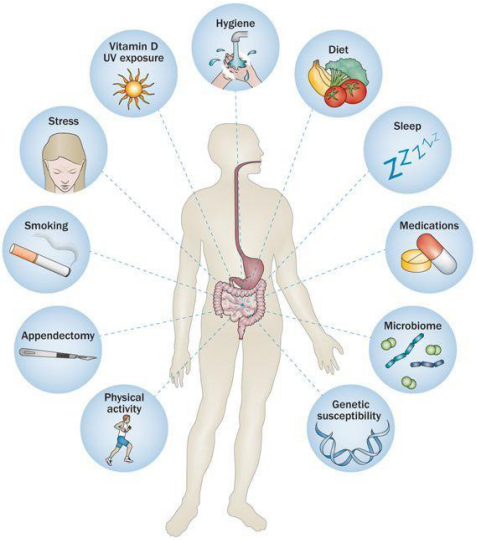

Figure 2. Risk factors, leading of development of IBD. From: Ananthakrishnan, A. N. Epidemiology and risk factors for IBD. Nat. Rev. Gastroenterol. Hepatol (2015)[13]

2.1.3 Genetics

Early family and twin studies have demonstrated that genetic factors play a fundamental role in disease susceptibility of IBD[13].

Genome-wide association study (GWAS), whole exome sequencing (WES), and fine-mapping have dramatically facilitated genetic research in IBD, identifying more than 240 susceptibility loci of IBD, including tumor necrosis factor (TNF) superfamily member 15 (*TNFSF15*),

interleukin 23 receptor (*IL23R*), autophagy related 16 like 1 (*ATG16L1*), immunity related GTPase M (*IRGM*), PR/SET domain 1 (*PRDM1*), and nuclear dot protein 52 kDa (*NDP52*, also known as *CALCOCO2*)[14, 15, 16]. Among these risk loci, some are shared by both CD and UC, while others are specific to one subtype (CD or UC). These data indicate that genetics plays a role in the pathogenesis of both CD and UC. However, it was quite disappointing to discover that the heritability conferred by genetic predisposition is smaller than expected (also known as missing heritability). Available data indicate that the portion of heritability explained by genetic variants was only 13.1% in CD, and 8.2% in UC[15].

Epigenetic modifications are defined as changes to gene structure and heritable phenotype that cannot be explained by altered DNA sequences. The classic epigenetic mechanisms include DNA methylation, histone modification, non-coding RNAs, and nucleosome positioning. In contrast, some new modifications such as RNA methylation are on the horizon[3, 17]. Among these modifications, DNA methylation and non-coding RNAs are most extensively studied in IBD research[1].

2.1.4 Gut microbiota

The human gut microbiota (GM) forms a complex community (bacteria, virus and fungi) that can influences the normal physiology and the susceptibility to disease[18]. Among them, bacteria, of which there are over 1000 different species, constitute the major part[19].

With the develop of next generation sequencing tools, the field of microbiota research took a leap forward. Population-scale studies have aided in understanding the functional consequences of microbiota remarkable inter-individual diversity, the earliest of which include MetaHIT (Metagenomics of the Human Intestinal Tract) and the Human Microbiome Project [19, 20]. More than 90% of healthy human gut bacterial species belong to four major phyla: Bacteroidetes, Firmicutes, Actinobacteria and Proteobacteria[21]. Microbial density increases distally, from the less favorable environment of the stomach, to the colon [22].

The human intestinal microbiota coevolves with its host through a symbiotic relationship and exerts great influence on substantial functions including aspects of physiology, metabolism, nutrition and regulation of immune responses leading to physiological homeostasis. Over the last years, several studies have been conducted toward the assessment of the host-gut microbiota interaction, aiming to elucidate the mechanisms underlying the pathogenesis of several diseases.

A defect on the microbiota-host crosstalk has been implicated in the pathogenesis of IBD. However, it is still controversial whether a specific individual bacterial species/strain or a group of certain bacterial species/strains might be causative of IBD or only contribute in exacerbation of IBD pathogenesis.

Several studies have demonstrated the high prevalence of specific bacterial pathogenic or commensal species/strains in IBD patients, but so far none of these species/strains could be convincingly shown to cause IBD[23]. This question has also been addressed in mouse models infected with enteric pathogens to evaluate the colitogenic potential of an individual specific bacterial species to cause chronic inflammation[24].

Under normal physiological conditions, GM acts as a homeostatic organ involved in the fermentation of complex undigested polysaccharide polymers, production of short-chain fatty acids (SCFAs), synthesis of certain vitamins, energy production, intestinal mucosa integrity, and preclusion of pathogenic microbes[25, 26, 27]. In addition, certain symbiotic gut microbiota members have been reported to have distinct and specific effects on the host immune system, and are considered key to immune homeostasis[28, 29].

The balance of Th17 and Treg cells, which are characterized by pro-inflammatory and anti-inflammatory cytokines, is critical for the host's intestinal homeostasis and is directly affected by the normal GM content. Evidence from

segmented filamentous bacteria (SFB) in mice has shown a high level of accumulation of pro-inflammatory cytokines of T helper 1 (Th1) and T helper 17 (Th17)[30,31]. Bacterial species from the *Clostridia* and *Bacteroides* genera induce anti-inflammatory and T-reg cell responses[32, 33]. Some other studies have reported that certain bacterial antigenic signals, such as the retinoic acid of *Clostridium* cluster IV and XIVa[34], polysaccharide A of *Bacteroides fragilis*[35] and *Faecalibacterium prausnitzii*[36] are involved in triggering an immune response and the accumulation of T-reg cells. The given mouse model studies suggest that gut microbiota play a role in mucosal immune homeostasis and inflammation, particularly in the Th17/T-reg balance, which is considered a dominant factor in induction and inhibition of colonic inflammation[37].

GM restoration is associated with an improved healthy status. The therapeutic supplementation of probiotics, prebiotics, and synbiotics, and fecal microbiota transplantation (FMT), all seek to alter the gut microbial community and restore a healthy composition in order to alleviate the pathophysiology associated with IBD[38].

2.1.5 Innate and adaptive immune system

The mucosal immune system, as a physical barrier, prevents pathogenic microorganisms and immunogenic components from traversing from the mucosae into the internal environment of the host. At the same time, this tightly regulated system has the important task of inducing tolerance to antigens[39].

Mucosal barrier function is regulated by various signals from gut microbiota and host immune cells.

Several types of innate immune cells have been shown to contribute to IBD pathogenesis (Figure 3). Innate lymphoid cells (ILC) are responsible for gastrointestinal mucosal homeostasis through moderate generation of IL-22, IL-17. Neutrophils perpetuate intestinal inflammation through impairment of the epithelial barrier function and release of multiple inflammatory mediators[40]. Dendritic cells (DCs) control crosstalk between the innate and the adaptive immunity to maintain homeostasis[41].

Particularly relevant are the intestinal epithelial cells (IECs) that include enterocytes, goblet cells, enteroendocrine cells, Paneth cells, M cells, cup cells, and Tuft cells, all of which differentiate from common epithelial stem cells[42].

Gut immune homeostasis is maintained by continuous sensing of microbial antigens by macrophages and DCs, but also epithelial cells and myofibroblasts. Sensing is mediated

by pattern-recognition receptors (PRRs), including toll-like receptors (TLRs) and NOD-like receptors (NLRs) that recognize pathogen-associated molecular patterns (PAMPs). PRR sensing and expression is highly regulated in order to maintain tolerance to commensal bacteria and prevent inappropriate immune responses[43,44]. Thus, it is not surprising that mutations in genes encoding TLRs and NLRs have been associated with IBD, such as NOD2 polymorphisms conferring risk for CD[45, 46, 47.]

In IBD patients, mucosal DCs and macrophages show an increased expression of TLR2, TLR4, CD40, and chemokine receptor CCR7 all of which contribute to and promote inflammation by inducing production of pro-inflammatory cytokines, such as TNF, interleukin (IL)-1β, (IL)-6, and (IL)-18[48, 49].

Among the pro-inflammatory cytokines, TNF, secreted by various immune and stromal cell populations, has been the star focus. This cytokine is considered to be responsible for amplifying and maintaining the chronic inflammation in IBD by promoting transcription of other pro-inflammatory cytokines, up-regulating adhesion molecules in the endothelium and activating phagocytic activity of macrophages[50].

Monoclonal antibodies (mAbs), such as infliximab (IFX), adalimumab (ADA), certulizumab pegol and

golimumab, all targeting TNF, have been successful at inducing clinical remission and effective for the treatment of active IBD lesions[51].

Other key cytokines of the innate immune system such as IL-6, reported to participate in sustaining T-cell survival signals, and IL-1β, involved in granulocyte recruitment and boosting of Th17 activity, could be potential therapeutic targets for IBD treatment[52].

While the innate immune system induces inflammatory responses, the adaptive immune system plays a central role in the progression of the chronic inflammatory events seen in IBD[53]. Naïve $CD4^+$ T-cells activated by antigen-specific signals from APCs, influenced by the cytokine milieu, differentiate into effector T-helper cells; T-helper 1 (Th1), T-helper 2 (Th2), T-helper 17 (Th17) cells, T-helper 9 (Th9), or regulatory T-cells (Tregs)[54]. The differentiation of naive $CD4^+$ T-cells into effector T-cell lineages has in the past been considered to be an irreversible event; however, certain cytokine conditions and stimuli may lead to plasticity between T-cell subsets[55].

The immune imbalance of Th1 and Th2 subsets has been shown to play an important role in IBD development. A Th1 dominated immune response, with high amounts of IL-2 and IFN-γ, has been seen to be more pronounced in CD patients as compared with UC patients[56]. The increased

mucosal level of the pro-inflammatory cytokine IFN-γ sequentially affects other immune cells such as intestinal macrophages to induce TNF production and in turn plays a crucial role in the amplification of disease chronicity in IBD[50]. In contrast, it has been shown that mucosal T-cells of UC patients release higher amounts of IL-5 and IL-13 than CD patients and controls[57, 58].

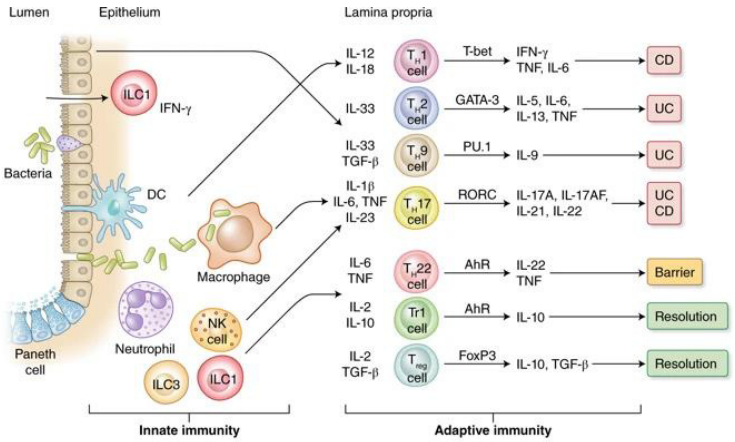

Figure 3. Immune cell subsets and cytokines in IBD. From: Neurath MF. Targeting immune cell circuits and trafficking in inflammatory bowel disease. Nat Immunol. (2019)[59].

2.1.6 Environmental factors

Despite the aforementioned advances, only about 25% of IBD heritability has been explained by genetic studies[60].

Furthermore, new epidemiological trends of IBD in developing countries following industrialization suggest that environmental factors may play an important role in promoting intestinal inflammation in genetically susceptible individuals[61].

Smoking has been one of the most studied factors in the setting of IBD. Clinically, cigarette smoking has been found to be harmful in patients with CD but protective to those with UC[62]. Different pathways have been hypothesized to explain these findings, including impairments of autophagy, direct toxicity to immune- and mucus-producing cells, and inducing changes in the microbiome[63].

Moreover, exposure to diets rich in saturated fatty acids and processed meats has been reported to increase the risk of IBD[64, 65]. Conversely, a high-fiber diet has been found to reduce the risk of CD by 40%[60].

The use of medications, most notably antibiotics, mainly during childhood, has also been associated with increased risk of IBD[66, 67]. This association usually results from changes in the intestinal microbiome after use of antibiotics during early stages of life, when the microbiota plays a critical role in shaping immune cell development[68].

Non steroidal anti-inflammatory drugs, anti-contraceptives, and statins are other examples of medications

that have been associated with up to 2-fold-increased risk for CD and UC[69, 70].

Early life events such as mode of delivery, breast-feeding, exposure to pets, and infections ("hygiene hypothesis") are also factors associated with considerable risk for development of IBD, mostly given influences in the composition of the intestinal microbiota[71, 72, 73].

2.2 The intestinal epithelial barrier

Epithelial barriers have to constantly cope with both harmless and harmful stimuli. The epithelial barrier therefore serves as a dynamic and not static wall to safeguard its proper physiological function while ensuring protection. This is achieved through multiple defence mechanisms involving various cell types - epithelial and non-epithelial - that work in an integrated manner to build protective barriers at mucosal sites.

The epithelial barrier consists of multiple layers of defence, which function both simultaneously and subsequently with each other. Geographically, from the outside (lumen) towards the inside (*lamina propria*): (1) the outer most layer consists of mucus which acts as a physical barrier (2) that is further reinforced biochemically with antimicrobial peptides and immunoglobulin A. (3) Intestinal epithelial cells (IECs) form a single-cell layer of protection which is interspersed

with intraepithelial lymphocytes. (4) Within intestinal crypts are intestinal epithelial stem cells, which are key in replenishing the epithelial surface. (5) Beyond the epithelial layer is the *lamina propria*, which is densely populated with leukocytes that serve to back up the innate immune defences and provide immunological memory against future repeated insults[74] (Figure 4).

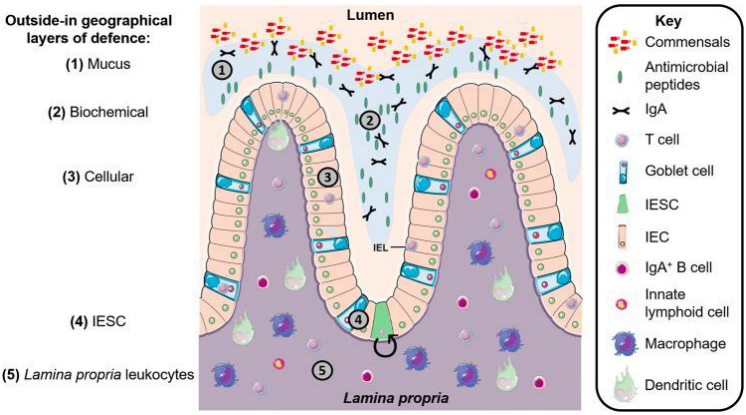

Figure 4. Geographical layers of intestinal (colon) defence mechanism. From: Thoo L. et al. Keep calm: the intestinal barrier at the interface of peace and war. (2019)[74].

Since intestinal barrier integrity is critically dependent on IECs fitness, mechanisms affecting IECs function are important parameters that regulate the epithelial barrier.

IECs and innate immune cells (such as tissue-resident macrophages and dendritic cells) sense microbial signals both

directly from the microbes and factors released by infected cells (pathogen-associated molecular patterns; PAMPs) via evolutionarily conserved PRRs, thereby initiating an inflammatory cascade inducing the secretion of cytokines and chemokines for the recruitment of myeloid immune cells[75].

IECs are among the first responders to microbes and express a wide range of PRRs ranging from extracellular and endosomal membrane-bound TLRs to cytoplasmic RIG-I-like receptors (RLRs) and NLRs, which enable the detection of microbial molecules[42].

Inflammation can also be induced by non-microbial stimuli, such as sterile cellular damage. Damage-associated molecular patterns (DAMPs), similarly to PAMPs, possess conserved molecular patterns recognised by PRRs expressed by IECs and several other cell types at mucosal sites. DAMPs are often intracellular components (e.g. nucleic acids, ATP) which are released by damaged or necrotic cells[76].

Once the epithelial barrier has been breached by pathogens or by physical or chemical insult, PAMPs/DAMPs activate IECs to secrete cytokines and chemokines, and tissue-resident myeloid cells to secrete lipid-derived mediators (e.g. prostaglandins and leukotrienes).

Inflammatory cytokines such as TNF and IFNγ can disrupt the epithelial barrier by downregulating tight junctions (claudin-1, occludin, zonula occludens protein-1)[77], and

adherens junctions (E-cadherin) in IECs[78] thereby compromising the physical barrier, one of the key "layers of defence" .

Despite its multifactorial aetiology, a characteristic of IBD is the disruption of the epithelial barrier, which allows unrestricted interaction of the commensal microbes with the IECs and the immune cells and therefore contributes to the sustained mucosal inflammation[79]. Repairing the barrier in IBD is therefore important to prevent damage from spreading faster than repair can occur.

2.3 HMGB Family

The HMG superfamily is divided into three families based on their DNA binding domains: the AT hook domain containing HMGA; the HMG box containing HMGB; and the nucleosomal binding domain containing HMGN proteins[80, 81].

The DNA structure-dependent interactions of these proteins are highly dynamic and affect both DNA and chromatin structures, thereby impacting processes such as DNA replication, transcription, and DNA repair[82, 83].

The HMGB proteins are highly abundant. These proteins bind the minor groove of DNA and have a characteristic domain structure consisting of a Box A N-terminal domain, a Box B central domain, and an acidic C-

terminal domain (Figure 5). It has been shown that the Box A domain binds DNA[84], the Box B domain binds and facilitates bending of DNA[85], and the C-terminal tail plays a regulatory role in the DNA binding and bending properties of the HMGB proteins[86].

2.3.1 DAMPs and HMGB1

The "Danger Theory" describes that our body has developed mechanisms to detect pathogens via recognition of molecules such as DAMPs triggering the immune system against various stimuli during physiological or pathological conditions. The 'danger model' refers to an immunity model which primarily aims at molecules causing damage rather than those that are foreign[87].

DAMPs are essential for tissue repair and play a crucial role in inflammatory and autoimmune conditions mainly through TLR activation[88].

The high mobility group box 1 (HMGB1) (Figure 5) protein is the only prototypical DAMP which functions as a typical alarmin and stimulates an innate immune mechanism either by itself or through interaction with cytokines and other exogenous or endogenous molecules[89, 90].

HMGB1 is a DNA binding protein recognized as a pro-inflammatory mediator in infection or sterile tissue injury,

with vital role in the orchestration of innate immune responses[91].

It is found in all mammalian tissues and is highly conserved between different species with 99% sequence homology among rodents and humans[92].

HMGB1 exists in 3 isoforms (fully reduced HMGB1, sulfonyl HMGB1 and disulfide HMGB1). However, disulfide HMGB1 is the only one exhibiting pro-inflammatory cytokine-like activity[93].

The biological activity of HMGB1 depends on its cellular location, context and post-translational modifications. The post-translational modifications of HMGB1 include primarily acetylation, phosphorylation, methylation, ADP ribosylation (PARylation, PARP1 mediated), and redox modification. Such modifications may alter the conformation of HMGB1, resulting in different biochemical properties[94].

Intracellularly, HMGB1 regulates the autophagic flux whereas in the nucleus, it contributes to an array of DNA-based events (repair, transcriptional regulation as well as genomic stability)[95].

In the extracellular milieu, it participates in a plethora of cellular activities depending on the oxidative status, such as inflammation, migration, invasion, proliferation, differentiation and tissue regeneration. Cytokine-like effects of extracellular HMGB1 have been widely recognized and

appreciated in recent years making it an attractive target against several HMGB1-mediated pathologies[96].

Furthermore, HMGB1 is actively secreted by various immune cells, especially monocytes and neutrophils in response to stimulation by endotoxin lipopolysaccharide (LPS), CpG DNA, TNF-α, and IL-1[97].

Nucleus-to-cytoplasmic translocation of HMGB1 and subsequent release into the extracellular space are crucial events for HMGB1-mediated inflammatory responses.
Extracellular HMGB1 displays its cytokine activities mainly via its interaction with several surface molecules, including RAGE, TLR2 and TLR4, thrombomodulin and syndecan[80].

In addition, it acts synergistically with a number of factors or pro-inflammatory molecules, such as single-stranded DNA, LPS, IL-1β and even nucleosomes from apoptotic cells, forming highly inflammatory complexes that are capable of binding to the above receptors, enhancing the activity of HMGB1[98].

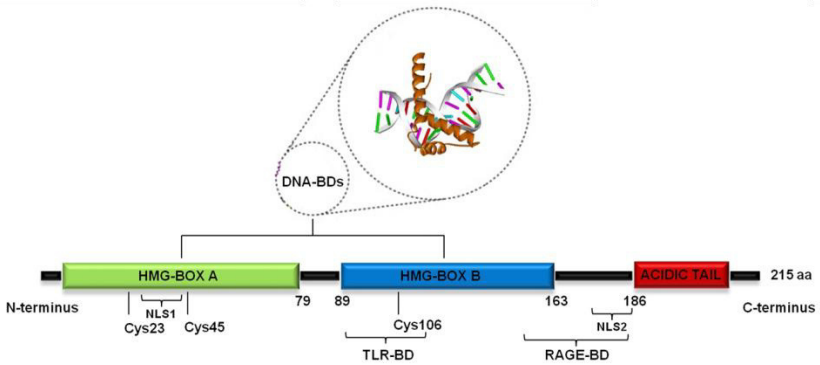

Figure 5. HMGB1 structure. HMGB1 is a 25 kDa nuclear protein of 215 amino acids. It comprises two DNA-binding domains, boxes A and B, and a negatively charged C-terminal tail (Acidic tail). The regions required for the activation of TLR and RAGE are respectively located between residues 90-105 and 150-183. (NLS, nuclear localization sites). From: Xu, T., *et al.* The progression of hmgb1-induced autophagy in cancer biology. Onco. Targets. Ther. (2019)[99]

2.3.2 HMGB1 and IBD

The role of HMGB1 in IBD pathogenesis has been further explored by analyzing HMGB1 expression in the colonic mucosa. In a mouse model of UC prepared with DSS, colonic expression of HMGB1 and its receptor, RAGE, were significantly higher than in control mice[100].

Application of anti-HMGB1 antibody prevented weight loss in DSS-treated mice, decreased inflammation, and limited permeability of colon[101].

In IL-10$^{-/-}$ mice, fecal HMGB1 levels were markedly elevated, but decreased after systemic ethyl pyruvate (EP)

treatment, whereas in TNBS intra-rectal treated mice, local delivery of EP also ameliorated colitis and reduced TNF production[102].

HMGB1 was found to promote inflammatory cytokines secretion by acting on TLR2/4 resulting in tissue damage[103].

In another study, the dipotassium glycyrrhizate (DPG), a salt of the glycoconjugated triterpene glycyrrhizin that has been shown to inhibit HMGB1, not only reduced fecal HMGB1 in DSS-treated mice and ameliorated colitis, but effectively downregulated RAGE and TLR4 mRNA, and downstream inflammatory cytokines TNFα , IL-1β , and IL-6[104]. More recently, DPG, by inhibiting HMGB1, was found to strongly accelerate mucosal healing by differently regulating pro-inflammatory and wound healing genes[105].

As shown above, fecal HMGB1 levels were elevated in models of both acute (like DSS and TNBS treatment) and chronic [IL-$10^{-/-}$ mice] colitis, and administration of HMGB1 antagonists, both systemically and locally, seem to ameliorate colitis, raising the prospect of a potential clinical treatment for IBD.

Finally, fecal HMGB1 has been suggested to be a novel noninvasive biomarker of gut inflammation, able to identify histologic inflammation in subjects with IBD in clinical and endoscopic remission[106].

2.4 PARP Superfamily

Poly(ADP-ribose) polymerases (PARPs), also known as ADP-ribosyltransferases (ARTs), are a family of proteins that play key roles in various biological processes[107, 108].

The PARP superfamily catalyzes either mono-ADP-ribose (MAR) or poly ADP-ribose (PAR) to target proteins using nicotinamide adenine dinucleotide (NAD^+) as a donor; this process is also termed MARylation or PARylation, respectively[109].

PARylation is a reversible process in which covalently linked PAR can be hydrolyzed to free PAR by PAR glycohydrolase (PARG) or PAR hydrolase (ARH3)[110].

Humans express at least 17 PARP enzymes that play important roles in regulating fundamental physiological processes in cells. Except for a splice variant of PARP13, PARP13.2, all other PARP members contain a classical PARP domain, which catalyzes ADP-ribosylation of target proteins[111].

2.4.1 PARP1: structure and function

PARP1 is the prototypical and founding member of the PARP family, which can be divided into three functional domains: (1) the amino-terminal DNA-binding domain l (DBD) contains three zinc-fingers, a nuclear localization

signal (NLS), and a caspase-3 cleavage site; (2) the central auto-modificationdomain (AMD) contains numerous glutamic acid and aspartic acid residues, which is consistent with the fact that it is the main site of PARP1 auto-modification. This domain also contains a breast cancer-susceptibility gene1 C-terminus (BRCT) motif, a protein-protein interaction motif, which is commonly found in proteins involved in DNA repair and control of the cell cycle[112] (Figure 6).

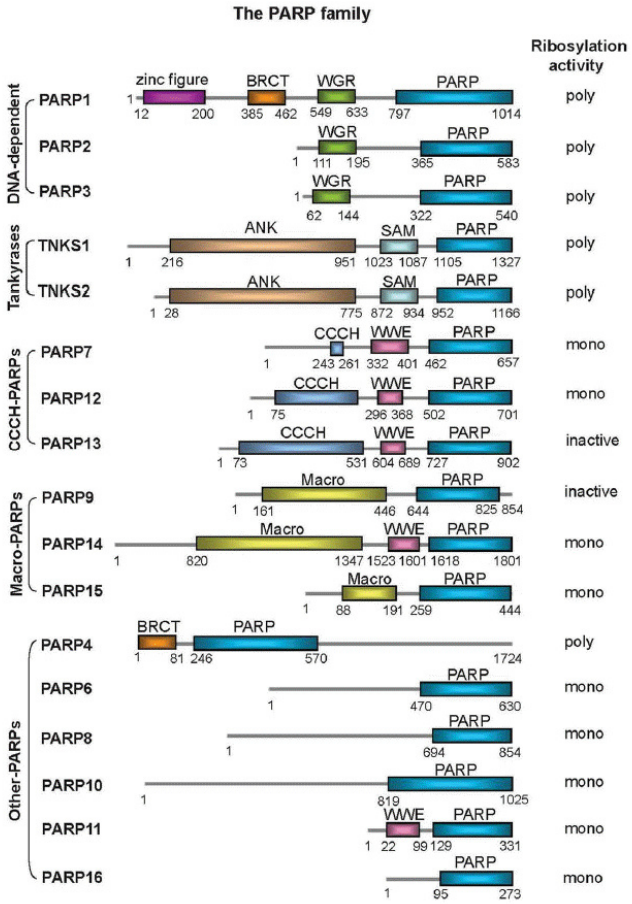

Figure 6. The domain organization of PARPs. The PARP domain is the catalytic domain and is required for NAD+ binding and PAR synthesis. The zinc finger domain is a DNA-binding domain. The BRCA1 C terminus (BRCT), ankyrin repeat (ANK) and sterile α-motif (SAM) domains are protein-protein interaction domains. The CCCH domain is a Cys-Cys- Cys-His zinc finger domain. The WGR is a functionally unknown domain. Macro and WWE are PAR-binding domains. From: Li, N., et al. ADP-Ribosylation: Activation, Recognition, and Removal. Mol. Cells. (2014)[113]

PARP1 is usually activated by DNA damage, and the modified target is primarily PARP1 itself, which is called PARP1 auto-modification. Furthermore, binding to non-damaged DNA structures is considered to be a valid determinant of PARP1 activation in the absence of abundant DNA fragmentation[114].

Actually, a large body of data has now shown that PARP1 functions as a cellular rheostat, promoting different cellular response upon a wide range of type, duration, and strength of stress signals[110].

2.4.2 PARP1 and inflammation

Given its role in cell death, PARP1 is thought to play a critical role in the inflammatory response *in vivo*. Necrotic cells can release a number of mediators that can induce the recruitment and activation of inflammatory cells such as neutrophils and monocytes. Mediators released by dying cells are referred to as DAMPs, a set of intracellular molecules with a well-defined physiological function, such as DNA, ATP, NAD+ or proteins like HMGB1, that act as inducers or amplifiers of an inflammatory reaction when released in the extracellular milieu[115]. Although a direct and conclusive demonstration for a role of DAMPs in mediating PARP1-induced inflammation is still lacking, several studies support

this contention. PARP1$^{-/-}$ mice or mice treated with nicotinamide can be protected from type 1 diabetes due to increased survival of β-cells and reduced inflammation[116].

A large array of data using PARP inhibitors also support a causal link between reduced PARP1 activity, increased cell survival and the resolution of inflammatory reactions[117].

Initial studies using knockout mice models showed that PARP1 is crucial for the expression of several pro-inflammatory cytokines after stimulation with microbial products such as LPS, and that PARP1$^{-/-}$ mice were protected from LPS-induced septic shock due to a defect in NFκB activation[118, 119].

The canonical NFκB transcription factor, a dimer of the p50 and p65 (RelA) subunits, is sequestered in the cytoplasm by inhibitory proteins of the IκB family. The phosphorylation of IκBα by the IκB kinase (IKK) complex leads to its degradation by the ubiquitin-proteasome system and to the release of the p50/p65 dimer which can be translocated into the nucleus and activate transcription[120].

The translocation of the NFκB p50/p65 dimer into the nucleus occurs normally in PARP1$^{-/-}$ mice, but its binding to DNA is greatly reduced, resulting in defective TNFα production and inducible Nitric Oxide Synthase (iNOS) expression in macrophages[118].

PARP1 also has a positive effect on other important immune-related transcription factors. PARP1 has indeed been shown to positively regulate among others the activator protein-1 (AP-1) in fibroblasts and Nuclear Factor of activated T-cells (NFATc1 and NFATc2) transcriptional regulators[121].

More recently, different studies have shown that the activation of PARP1 regulates the translocation of HMGB1 from the nucleus to the cytosol[122]. PARP1 mediates HMGB1 release through its PARylation. PARylated HMGB1 is mainly secreted by cells stimulated through TLR4 engagement[123]. During LPS-induced inflammation, PARylation of HMGB1 is necessary but not sufficient to nucleus-cytoplasm translocation, indeed, the PARylation of HMGB1 promotes the acetylation of HMGB1 and then its release from the nucleus[122]. A recent study highlights that the functional inhibition between PARP1 and the deacetylase Sirtuin1 (Sirt1) leads to HMGB1 hyperacetylation, which leads to its translocation from the nucleus to the cytoplasm and finally outside the cell[124].

PARP1 inhibition mitigates morbidity and mortality in multiple inflammatory, immune mediated and autoimmune diseases such as diabetes mellitus, rheumatoid arthritis, septic shock, ischemic stroke, acute pancreatitis, asthma, and inflammatory bowel disease-like colitis[125].

Genetic ablation or pharmacological inhibition of PARP1 reduces the biological and physical manifestations of experimental colitis[126,127]; IL-10$^{-/-}$ mice treated with a PARP1 inhibitor (3-aminobenzamide) show a significant reduction in proinflammatory cytokine production associated with reduced intestinal permeability[128].

Other PARP1 inhibitors have also been used successfully to prevent hapten-induced colitis in rats[129,130] and in mice[131, 132].

The efficacy of PJ34, a novel, potent phenanthridinone derivative PARP inhibitor, in rodent models of diabetic vascular dysfunction and stroke and in local inflammation model has been demonstrated[130]. Furthermore, PJ-34 was suggested to exert its protective effect on intestinal epithelial cells against invasive Salmonella infection by up-regulating IL-6 production through ERK and NF-kB but not P38 MAPK, JNK or PI3K/Akt signal pathways[133].

2.5 3D cultures as an innovative method to study the physiopathology of the gut

Recently, remarkable progress has been made in long-term primary IEC cultures called human intestinal enteroids (small intestine) and colonoids (colon)/colonoids which develop from human adult intestinal stem cells (ISCs)[134, 135].

Ex vivo human enteroid/colonoid cultures have diverse advantages over traditional animal models and cell lines in context of recapitulating human *in vivo* physiology, even after many generations, apparently with limited genetic or physiologic alterations[136].

In contrast to cancer cell lines which are genetically transformed and thus represent altered genotypes and phenotypes significantly different from those of primary cells[137], the intestinal enteroid/colonoid culture is a primary culture system which maintains *in vivo* characteristics of human intestinal epithelium even after many passages [134].

Furthermore, the current human cancer derived intestinal epithelial cell lines, as normally grown, consist of a single cell type (*e.g.*, Caco-2, HT29: enterocyte)[138, 139] and thus fail to recapitulate the diversity of cell types in the normal intestinal epithelium. Differently, intestinal enteroids/colonoids can give rise to all types of epithelial cells in crypt or villus structure (ISCs, Paneth cells, transit amplifying cells, enteroendocrine cells, goblet cells, enterocytes, tuft cells, and microfold cells)[140, 141]. Thus, intestinal enteroids/colonoids can more closely reflect normal physiology or disease pathogenesis of intestinal epithelium where each single type of IECs interact with other types of IECs by paracrine and autocrine mechanisms[142].

Additionally, intestinal enteroids/colonoids can be easily established from endoscopic biopsies in IBD patients and maintain the location or some disease specific features[143,144]. Colonoid development was allowed by the discovery of the Leucine Rich Repeat Containing G Protein-Coupled Receptor 5 (LGR5), a marker of ISCs (Figure 7).

Therefore, despite some limitations (e.g. a lack of mesenchymal tissue, immune and neural cells and presence only of a specific epithelial niche of self-renewal intestinal stem cells), the intestinal enteroid/colonoid culture system represents a promising tool for IBD modeling and drug development focusing on IEC dysfunction.

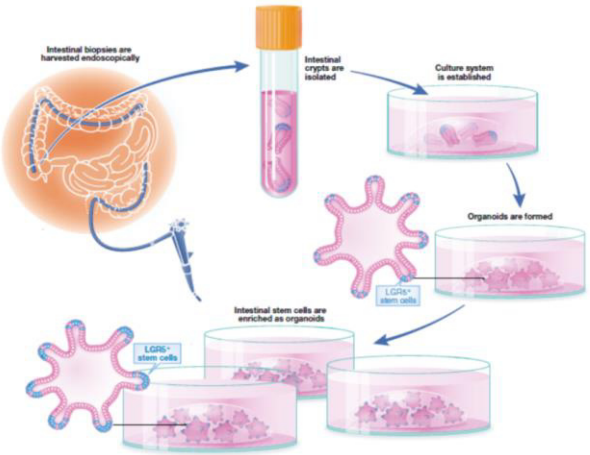

Figure 7. Intestinal colonoid cultures. From: Holmberg et al. Culturing human intestinal stem cells for regenerative applications in the treatment of inflammatory bowel disease. EMBO Mol. Med. (2017)[145]

3. AIMS OF THE STUDY

HMGB1 exhibits various functions according to its subcellular location, which is finely conditioned by diverse post-translational modifications.

Recent evidences suggest that PARP1 induce the poly-ADP-ribosylation (PARylation) of HMGB1 and regulates its translocation to the cytoplasm in some human cells.

The aim of this study was to investigate *in vivo* the relationship between PARP1 and HMGB1 in controlling intestinal inflammation by using PARP1 $^{-/-}$ mice.

Furthermore, cultures of intestinal colonoids from uninflamed colonic tissues of patients with UC were set up to deeply investigate the role of PARP1 and HMGB1 in gut inflammation.

Finally, the strategy to use a PARP1 inhibitor to limit the release of the pro-inflammatory extracellular HMGB1 was explored.

4. MATERIAL AND METHODS

4.1 Animals

C57BL6/J WT and PARP1 $^{-/-}$ female mice (8–9 wk of age) have been provided by Italian National Agency for New Technology, Energy and Sustainable Economic Development (ENEA). Mice were housed in collective cages at 22° ± 1° C under a 12-hour light/dark cycle and with food and water provided ad libitum. The experimental procedures were previously approved by the Ministry of Health for the protection of animals used for experimental purposes, and the study was conducted in accordance with Italian regulations on animal welfare. The protocol was approved by the Committee on the Ethics of Animal Experiments of ENEA.

4.2 *Animal treatment*

To induce colitis WT and PARP1 $^{-/-}$ mice (5 animals per group) were treated with 3% of dextran sodium sulphate (DSS; molecular mass, 36,000–50,000 Da, MP Biomedicals, Santa Ana, California) dissolved in drinking water ad libitum for 7 days. Mice were daily checked for the clinical score by assessing the following parameters: behavior, body weight, stool consistency (0 for normal stool, 1 for moist/sticky stool, 2 for soft stool, and 3 for diarrhea), presence of blood in stools

(0 for no blood, 1 for evidence of blood in stools or around anus, and 2 for severe bleeding), and general appearance of the animal (0 was assigned if normal, 1 for ruffled fur or altered gait, and 2 for lethargic or moribund), according to Maxwell *et al.* [146]. The percentage of weight loss was calculated in relation to the starting weight using the formula:

([Weight on day X - Initial weight]/Initial weight) X 100. Stool specimens were collected everyday and frozen at -80°C before analysis. Mice were euthanized on the seventh day, colons were weighed, and lengths were measured (from the anus to the top of the cecum). Distal colon was cut longitudinally and a small piece was frozen in liquid nitrogen for Western Blot analysis and RNA extraction and an other piece fixed for histology examination. Blood samples from submandibular vein were collected from each animal and stored at -80°C.

4.3 Histology

Distal colon samples were fixed in 10% formalin and embedded in paraffin for routine histology. To produce the histological score, fixed colon tissues were transversally sectioned (4µm thickness), mounted on glass slides, deparaffinized, and stained using standard Hematoxylin and Eosin techniques. Sections were analyzed by light microscopy

and scored according to the criteria of Maxwell *et al.*[146] Experiments were carried out in blind.

4.4 Human biopsy collection and ethical statement

Mucosal biopsies from macroscopically non-inflamed colon were obtained during routine endoscopy from UC patients at the University Hospitals Leuven (Table 1). The biopsies were collected in ice-cold basal medium (DMEM:F12 1:1 (Lonza, Basel, Switzerland) supplemented with 1X GlutaMAX (Gibco, ThermoFisher Scientific, Waltham, Massachusetts, USA) 10mM HEPES (Gibco) and 100U/ml+100µg/ml penicillin/streptomycin (Gibco), and processed within two hours for crypt isolation. All patients gave written informed consent before sample collection (approved by the Ethics Committee of the University Hospital Leuven – study number S53684).

Gender	Male	Female	Female	Male	Male	Male
Disease	UC	UC	UC	UC	UC	UC
Date of Diagnosis	15/07/2001	15/07/1989	05/07/2011	22/01/1996	15/03/2005	15/07/1989
Date endoscopy	06/11/2018	29/01/2019	05/02/2019	05/02/2019	26/02/2019	26/02/2019
Age at endoscopy	36,17	51,33	58,5	54,83	65,34	61,31
Disease duration	17,31	29,54	7,59	23,04	13,95	29,62
Location of disease (at diagnosis)	E3	E3	E2	E3	E3	E2
Location of disease (current)	fully cured colon	fully cured colon	fully cured colon	fully cured colon	fully cured colon	fully cured colon
Endoscopic disease activity	0	0	0	0	0	0

Table 1. Endoscopic disease activity assessment: UC = Mayo score

4.5 Intestinal crypt isolation and colonoid culture

Intestinal crypts were isolated from 4-6 colon biopsies per individual. In short, biopsies were washed in chelating solution (CS), which consists of distilled water with 5.6 mmol/L Na2HPO4, 8.0 mmol/L KH2PO4, 96.2 mmol/L NaCl, 1.6 mmol/L KCl, 43.4 mmol/L sucrose, 54.9 mmol/L D-sorbitol, 0.5 mmol/L DL-dithiothreitol. Biopsies were washed by 10x rigorously pipetting, changing CS 5-10x until the supernatant was clear (pipettes were pre-wet with foetal bovine serum (FBS) to prevent adhesion of biopsies to pipet). After, biopsies were incubated in CS containing 2 mmol/L EDTA for 45 minutes on a rocking platform at 4°C. EDTA containing CS was then removed and fresh CS was added. Biopsies were then subjected to rigorous pipetting to create four crypt-containing fractions of 10 ml each, which were

pooled after evaluation under a microscope. 10 ml FBS was added and crypts were spun down at 1200 RPM (150-200 *g*). Supernatant was removed and crypt were resuspended in Matrigel (Growth Factor Reduced, phenol-red-free, Corning NY, USA) diluted with basal medium (50/50%). To allow the formation of 3D colonoid structures, four droplets (10µl/drop) of each cell suspension were plated in every well of a 24 tissue culture plate. After polymerization, 500µl human expansion medium (HM) (WNT3A 50% v/v (in house, cell line), R-spondin-1 20% v/v (in house, cell line), Noggin 10% v/v (in house, cell line), EGF 50ng/ml (Life Tecnologies, Carlsbad, CA, USA), A83-01 500nM (Tocris Bioscience, Bristol, UK), SB202190 10µM (Sigma-Aldrich, Saint Louis, USA), Nicotinamide 10mM (Sigma), n-Acetylcysteine 1.25 mM (Sigma), B27 1X (Life Technologies) was added to the wells. Colonoid was refreshed every 2-3 days, and the colonoids were split after 7-10 days.

4.6 *Colonoid treatments*

Colonoids were seeded in 4 drops, 10µl each, in 24 multiwell plates. Induction of inflammation were performed by adding to 500µl HM medium TNFα and INFγ (Invitrogen) (Cytomix) at different concentration, 250ng, 150ng and 50ng (1:1) to evaluate the inflammatory

state and optimal working concentration, for 24 hrs. In a second set of experiment colonoids were co-treated with Cytomix 150ng and the PARP1 inhibitor, PJ34 at the following concentrations 200μM, 100μM and 50μM dissolved in DMSO, for 24 hrs.

4.7 Real-time Polymerase Chain Reaction

Total RNA was extracted from mouse colonic tissues and collected colonoids with the RNeasy kit (QiaGen GmbH, Hilden, Germany), and 1μg of total RNA was reverse transcribed by a High-Capacity cDNA Reverse Transcription Kit (Applied Biosystems, Foster City, CA) for colonic tissue and SuperScript™ III First-Strand Synthesis SuperMix (Invitrogen) for colonoids.

Real-time polymerase chain reaction was carried out with an ABI PRISM 7300 Sequence Detection System using the SYBR Green kit (Applied Biosystems). The primers were identified using the Primer Express v.3.0 (Applied Biosystems) provided with the ABI Prism 7300 sequence detector. Primers are enlisted in Table 2.

Messenger RNA (mRNA) levels were normalized to those of GAPDH for mice samples and to those of *RPS14*, *HPRT1*, and *B2M* for colonoids by the 2-ΔΔCT method. The expression

level of each mRNA was reported as folds of induction as respect to controls. *In vitro* experiments were repeated 3 times.

Table 2.

Symbol	Gene name	Forward	Reverse
hRPS14	*Ribosomal Protein S14*	TCACCGCCCTACACATCAAAC	GCCCGATCTTCATACCCGA
hHPRT1	*Hypoxanthine Phosphoribosyltransferase1*	GAAAAGGACCCCACGAAGTGT	AGTCAAGGGCATATCCTACAACA
hB2M	*Beta-2-Microglobulin*	TGCTGTCTCCATGTTTGATGTATCT	TCTCTGCTCCCCACCTCTAAGT
mGAPDH	*Glyceraldehyde phosphate dehydrogenase*	AACTTTGGCATTGTGGAAGG	CACATTGGGGGTAGGAACAC
hTNF-a	*Tumor necrosis factor- α*	ATCTTCTCGAACCCCGAGTGA	GGAGCTGCCCCTCAGCTT
hIL-1b	*Interleukin-1β*	TTCGACACATGGGATAACGAGG	TTTTTGCTGTGAGTCCCGGAG
hIL-8	*Interleukin-8*	TTGGCAGCCTGATTTC	TTGGAGTATGTCTTTATGCACTGAC
hDuoxa2	*Dual oxidase maturation factor 2*	TCCGCAACGATGGACAGA	AGGGTCGGTTGGAAACGAA
hHMGB1	*High Mobility Group B*	GCCTCGCGGAGGAAAATC	AAGTTTGCACAAAGAATGCATATGA

4.8 Preparation of protein extract and lumen content of colonoids

Colonoids were collected in ice-cold basal medium, after mechanically disaggregation were centrifuged at 800rpm for 10 min, the supernatant, containing the lumen content was collected for western blot. Colonoid pellets were suspended in ice-cold lysis buffer (50mM Tris (pH 7.4), 5mM EDTA, 250mM NaCl, 0.1% Triton X-100, 1mM phenylmethylsulfonyl fluoride, 5 mg/ml aprotinin, 5 mg/ml leupeptin, and 1mM sodium orthovanadate (Sigma), and incubated in ice for 30min. Samples were centrifuged at 14,000 r.p.m. for 10min., supernatants collected and analyzed by western blot. Total protein concentration was determined by the Bradford assay (Bio-Rad Laboratories, Hercules, CA).

4.9 Immunoblot Analysis

Fecal extract, protein extract of colonoids (10μg for HMGB1, and 30μg for PARP1), colonoid culture medium (25μl) and lumen content (25μl) were fractionated by sodium dodecyl sulfate-polyacrylamide gel electrophoresis to detect selected proteins. Proteins were transferred in polyvinylidene fluoride membrane (Bio-Rad) and blocked with TBS-T (Tris-buffered saline with Tween-20) containing 5% non-fat dry

milk. Anti-HMGB1 (1:1000; R&D system; Sigma), anti-PARP1 (1:1000; Cell Signaling), anti-b-actin (1:5000; Sigma) antibodies were diluted in TBS-T containing 3% non-fat dry milk and incubated overnight at 4 ◦ C. Membranes were washed in TBS-T, incubated for 1 h with horseradish peroxidase-conjugated secondary antibody (Santa Cruz Biotechnology Inc.,), washed in TBS-T, and developed with ECL-Plus (GE Healthcare, Life Science). Densitometrical analyses of the blots were performed using the Software ImageQuant (GE Healthcare, Life Science).

4.10 Quantification of Serum HMGB1 by Enzyme-linked Immunosorbent Assay

Murine serum HMGB1 levels were analyzed using the HMGB1 enzyme-linked immunosorbent assay (ELISA) kit (MyBioSource and EMELCA Bioscience, Breda, the Netherlands); samples were diluted (1: 200), in the kit recommended diluent buffer.

4.11 Fecal Extraction

Murine stool specimens, stored at -80°C, were resuspended in extraction buffer (ScheBo Biotech AG, Giessen, Germany) to a final concentration of 500 mg/mL.

Samples were vortexed for 1 minute at room temperature and placed in orbital shaking for 1 hour at room temperature. After being centrifuged twice for 5 minutes at 10,000 rpm at 4°C, clear supernatants were collected and stored at -80°C. Total protein concentration was determined by the Bradford assay (Bio-Rad Laboratories, Hercules, CA).

4.12 Statistics

All statistical analyses were performed with GraphPad InStat software (GraphPad Software, San Diego, CA, USA). The Kolmogorov–Smirnov test was used to assess whether data were sampled from populations following the gaussian distribution. Comparison among groups was performed using the Kruskal-Wallis Test with Dunn's Multiple Comparisons post-test.

For *in vitro* studies, all experiments were repeated three times and data were given as mean ± standard deviation (SD).

Comparisons among groups were performed by Mann–Whitney test. Differences were noted as significant ∗ $P < 0.05$, ∗∗ $P < 0.01$, ∗∗∗ $P < 0.001$.

5 RESULTS

5.1 PARP1$^{-/-}$ mice treated with 3% DSS developed a less severe colitis as compared to WT mice

PARP1$^{-/-}$ and WT mice (5 animals per group) were treated with DSS 3% for 7 days, to induce a severe colitis. The onset of colitis was confirmed by macroscopic (animal weight, colon length, clinical score) and microscopic (histology) endpoints. Results showed that PARP1$^{-/-}$ mice exhibited a less severe colitis compared to WT mice, as evidenced by less weight loss (*P < 0.05), higher clinical score value (*P < 0.05) and colon length (**P <0.01), (Figure 1A, B, C). Accordingly, histology showed an improved morphology of the intestinal mucosa and a significant reduction of the histological score (**P < 0.01) in PARP1$^{-/-}$ compared to WT mice (Figure 1 D, E).

Overall, our data highlights that the absence of PARP1 is protective against the onset of colitis induced by DSS 3%.

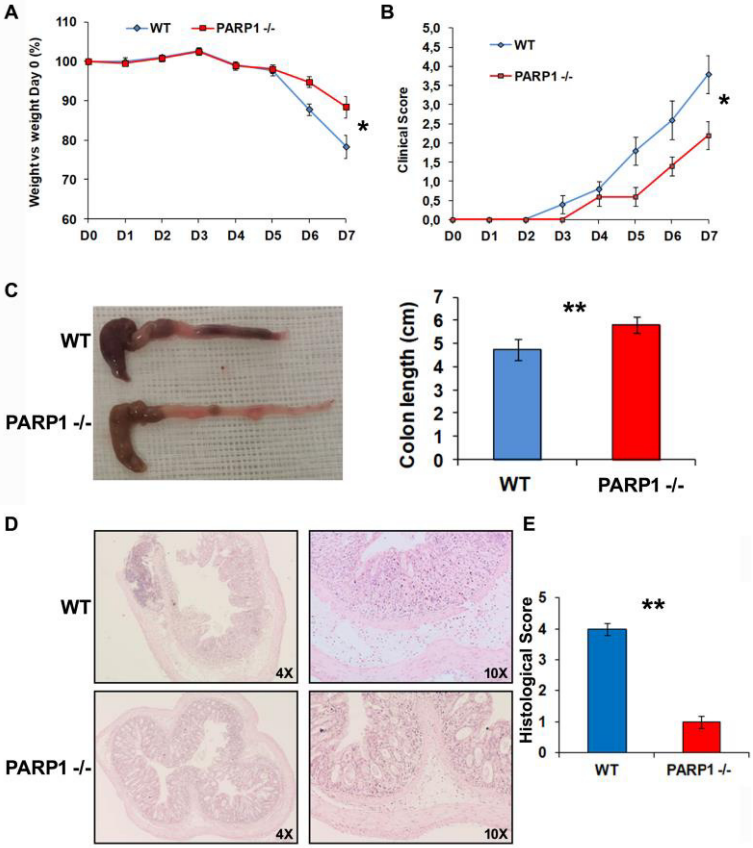

Figure 1. PARP1$^{-/-}$ vs WT mice A) Weight B) Total clinical score, C) Colon length, D) Histology, E) Histological score.

*P < 0.05; **P < 0.01

5.2 Extracellular HMGB1 is significantly reduced in the stools and serum of PARP1$^{-/-}$ as compared to WT mice, during colitis.

The mRNA expression of HMGB1 was analyzed after 7 days of treatment with DSS 3% by Real Time-PCR. As expected, HMGB1 mRNA expression does not vary between inflamed colonic tissues of PARP1$^{-/-}$ and WT mice (Figure 2 A).

Differently, the extracellular release of HMGB1 was analysed in both serum and stool samples of PARP1$^{-/-}$ and WT mice by ELISA and immunoblotting, respectively.

Results showed that HMGB1 levels were significantly decreased in the serum and stool samples of PARP1$^{-/-}$ as compared to WT mice (Figure 2 B, C).

These data suggest a relationship between PARP1 and HMGB1.

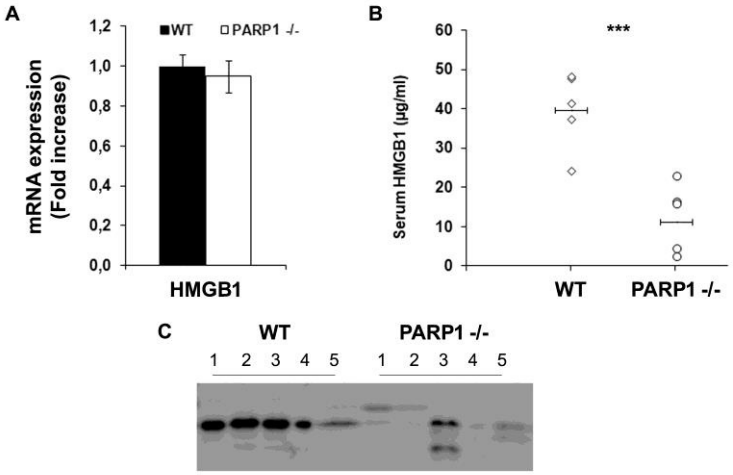

Figure 2. Analysis of HMGB1 after DSS treatment A) HMGB1 mRNA levels in colon tissue, B) Serum HMGB1, C) Fecal HMGB1. ***P < 0.001

5.3 Set up of human intestinal colonoids and analysis of active PARP1 and secreted HMGB1 during inflammation

We set up 3D cultures of intestinal colonocytes taken from the uninflamed areas of patients with UC, as an innovative method to study the pathogenesis of human gut inflammation.

Colonoids were treated with different doses of a mix of proinflammatory cytokines (cytomix: INFγ+TNFα) for 24 hours. Results showed that the highest dose (250 ng/ml; 1:1) of cytomix caused a dramatic decrease of cell viability, while

the lower doses (150 and 50 ng/ml, 1:1), produced viable colonoids (Figure 3 A). After 24 hours, the activation of PARP1 and the protein expression of HMGB1 were evaluated.

Results showed that the treatment with cytomix promoted the cleavage, thus the activation, of PARP1, as confirmed by the increase of the two PARP1 cleaved isoforms (89 and 55 kDa) in the protein extracts of colonoids. Indeed, as expected, HMGB1 protein expression did not vary nor intracellular nor released in the culture medium (Figure 3 B).

The colonoid structure is characterized by an internal lumen (Figure 3 C top), where the secretion of HMGB1 likely occurs. To analyze the secretion of HMGB1, colture medium was removed, colonoids were collected in basal medium and vigorously pipetting to induce lumen content release. Then samples were centrifuge and the supernatant (lumen content) was analyzed by immunoblotting. Results showed that HMGB1 is increased in the lumen, after the exposure of colonoids to the two higher cytomix concentrations (Figure 3 C bottom).

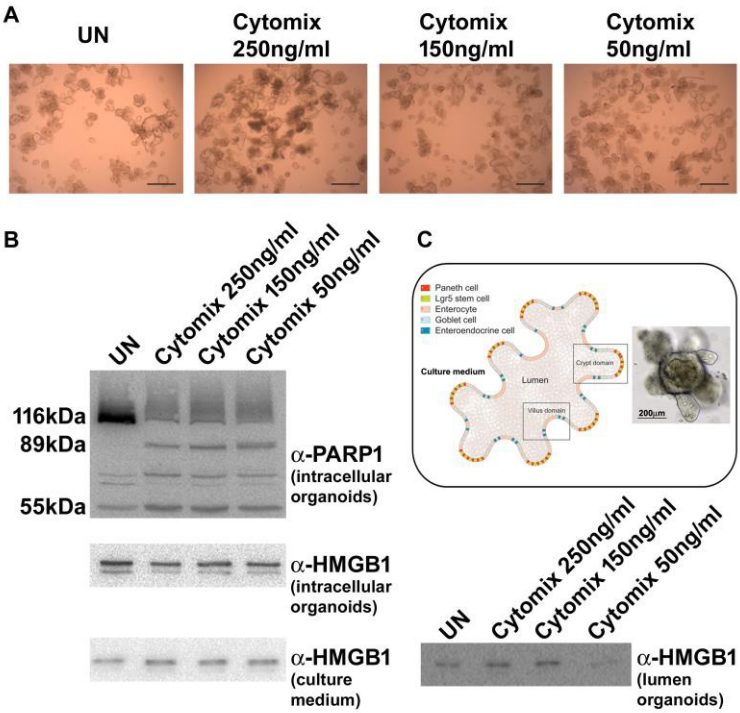

Figure 3. Set up of intestinal colonoids and treatment with cytomix**.** A) Viability and morphology (scale bar = 200µm); B) Western-blot analysis; C) Representative image of human intestinal colonoid and western-blot analysis of HMGB1 released in the colonoid lumen. (Modified by Lukova & Roeselers, Chap 22 in The Impact of Food Bioactives on Health. Springer Intl Publishing, 2015)[147]

5.4 PARP1-inhibitor, PJ34, reduces the release of HMGB1

PJ34 is a specific inhibitor of PARP1. We treated colonoids with the cytomix (150 ng/ml) alone or with the cytomix plus two different doses (100 or 200 μM) of PJ34. Again, colonoids were collected, vigorously pipetting and the lumen content was recovered for the analysis of the secreted HMGB1. Results showed that the lower dose of PJ34 inhibited the release of HMGB1 (Figure 4 A, B). Differently, the higher dose of PJ34 caused cytotoxicity and cell death of colonoids, as observed at the microscope (data not shown).

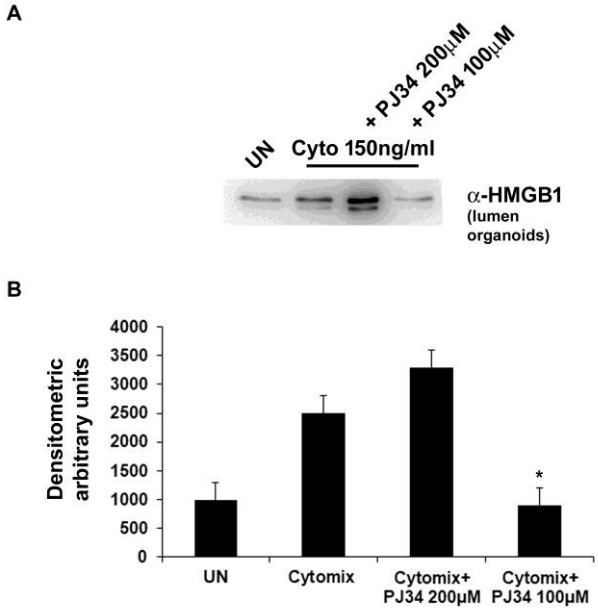

Figure 4. Colonoids treated with PARP1-inhibitor, PJ34, A) Western-blot of HMGB1 in the lumen content of colonoids; B) Densitometry. P is referred to comparison between cytomix+PJ34 100μM vs cytomix

5.5 Analysis of inflammatory and oxidative stress mediators in colonoids

Colonoids were exposed to the cytomix (150 ng/ml) alone or co-exposed to cytomix and PJ34 (100 μM). Then, the analysis of the expression of pro-inflammatory cytokines, IL-1β, IL-8, and TNFα as well as that of the stress oxidative enzyme dual oxidase maturation factor 2 (DUOXA2) was performed through Real Time-PCR. Results showed that

cytomix up-regulated the mRNA expression of all molecules analyzed, however, PJ34 significantly reduced only TNFα and DUOXA2 levels (Figure 5). This data suggest a preferential way of PJ34 to repress inflammation.

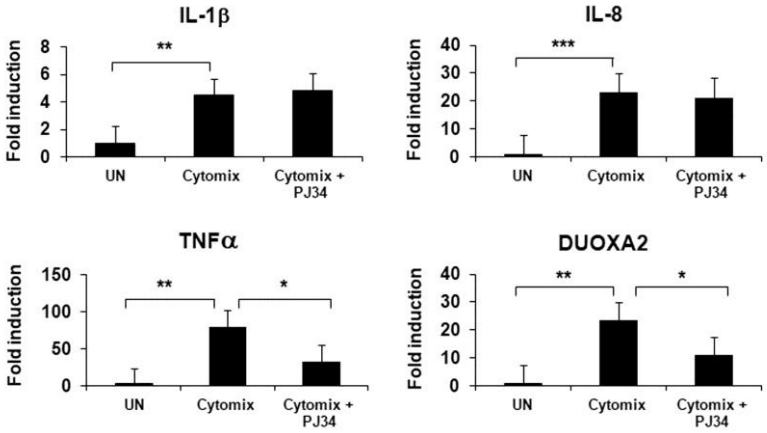

Figure 5. Gene expression of pro-inflammatory cytokines and DUOXA2 (oxidative stress) in colonoids *P < 0.05; **P < 0.01; ***P < 0.001

5.6 Induction of inflammation in differentiated colonoids

We have used the protocol to induce differentiation in colonoids and verify if differentiated colonoids respond to the inflammatory stimulus such as those not differentiated. Thus, in order to start the differentiation process, WNT3A, nicotinamide and p38-inhibitor were removed from the culture medium. Differentiated colonoids were morphologically

distinguishable from those not differentiated already from the second day; differentiation was completed at the fourth day (Figure 6 A).

Differentiated colonoids (day 4) were exposed for 24 hours to two different doses of cytomix (150 and 50 ng/ml) to induce inflammation. Results showed that mRNA expression of pro-inflammatory cytokines IL-1β, IL-8, TNFα and the oxidative stress gene DUOXA2 were significantly increased after cytomix exposure, this effect is not in dose dependent manner (Figure 6 B).

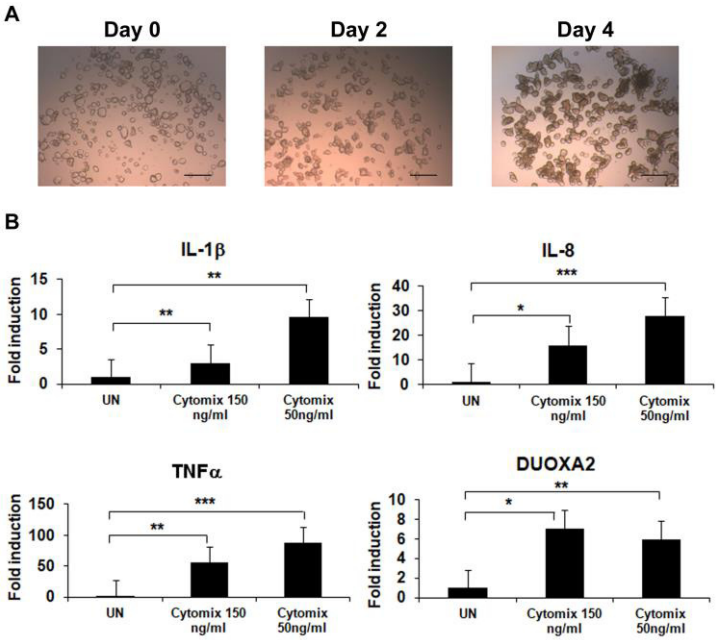

Figure 6. Induction of inflammation in differentiated colonoids. A) Morphology (scale bar = 200µm); B) mRNA expression of cytokines and DUOXA2. *P < 0.05; **P < 0.01; ***P < 0.001

5.7 PJ34 reduces the release of HMGB1 from differentiated colonoids

Differentiated colonoids (4 day) were exposed for 24 hours to two different doses of cytomix (150 and 50 ng/ml) and PARP1 cleavage (in colonoids) and extracellular HMGB1 secretion (in the lumen content) were analysed. Results showed that PARP1 was cleaved after both doses of cytomix.

Moreover, the higher dose of cytomix caused a significant release of HMGB1 (Figure 7 A). Then, we co-exposed differentiated colonoids to the higher dose of cytomix and three different doses of PJ34 (200-100-50 μM). Results showed that the lowest dose of PJ34 significantly decreased the release of HMGB1 (Figure 7 B). The release of HMGB1 observed at the highest dose of PJ34 is probably due to its cytotoxic effect.

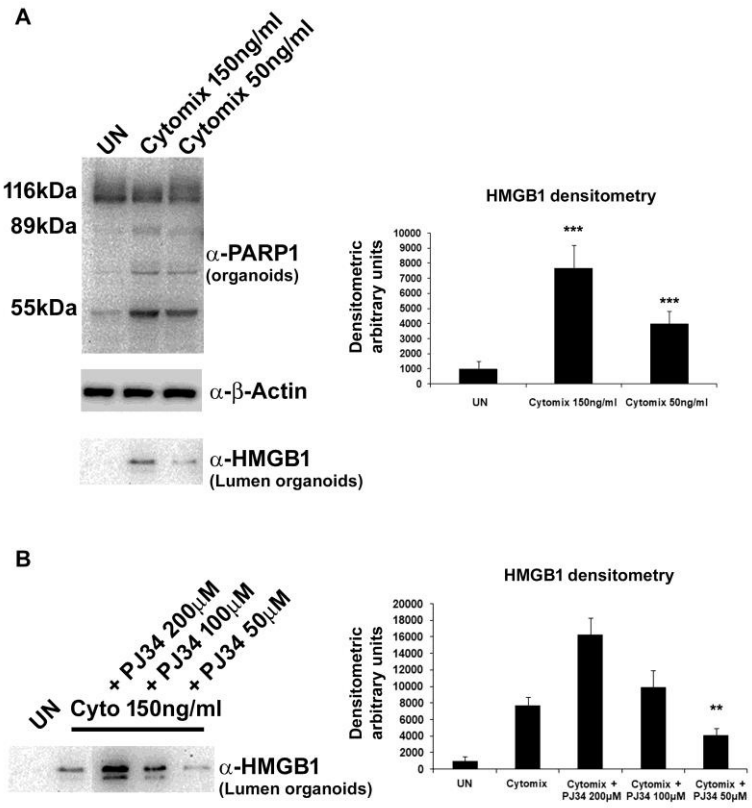

Figure 7. Differentiated colonoids treated with cytomix and PARP1 inhibitor, PJ34. A) Western-blot of PARP1 (in colonoids) and extracellular HMGB1 secretion (in the lumen content). Densitometric analysis of HMGB1 release is showed, P is referred to comparison between cytomix vs UN. B) Western-blot of extracellular HMGB1 secretion (in the lumen content) after PJ34 treatment. Densitometric analysis of HMGB1 release is showed, P is referred to comparison between cytomix+PJ34 vs Cytomix. **P < 0.01; ***P < 0.001.

6 DISCUSSION

IBDs are associated with multiple pathogenic factors including environmental changes, an array of susceptibility gene variants, a qualitatively and quantitatively abnormal gut microbiota and a broadly dysregulated immune response. In spite of this realization, a full understanding of IBD pathogenesis is still out of reach and, consequently, treatment is far from optimal. An important reason for this unsatisfactory situation is the currently limited comprehension of what are the truly relevant components of IBD immunopathogenesis.

However, substantial progress has been made in the understanding of IBD immunopathogenesis during the past few decades. In particular, HMGB1, a nuclear non-histone DNA-binding protein, has been proven to be released into the extracellular milieu and mediates inflammatory responses, strongly contributing to the pathogenesis of numerous inflammatory diseases, including IBD. More recently, the relationship between PARP1 activity and inflammation has been widely investigated. The link with inflammation was firmly established by the pharmacological inhibition of PARP1 activity, which allowed the attenuation of the inflammation response. The mechanisms underlying this effect imply also a role of PARP1 in regulating inflammatory factors.

Novel evidence showed a possible interaction between HMGB1 and PARP1, for example, suggesting that PARP1 may combine with HMGB1, accelerating its translocation from nucleus to cytoplasm. However, these studies were focused in other districts than the gastrointestinal one, where indeed the role of HMGB1 has been much investigated in the last years.

In this frame, this study aimed at exploring a possible relationship between HMGB1 and PARP1 in regulating intestinal inflammation. For this purpose, we first used mice knock out for PARP1, which were treated with the DSS to induce severe colitis and showed that they developed a less severe colitis than WT mice, as evidenced by macroscopic as well as histologic end-points. More interestingly, $PARP1^{-/-}$ mice exhibited a significant reduction in serum and stools levels of HMGB1, typically secreted by cells during the inflammatory processes. Remarkably, the presence of HMGB1 in the fecal stream has been previously correlated with the occurrence and the severity of gut inflammation[106].

These data clearly indicate that the ablation of PARP1 is linked to the release of HMGB1.

To deeply investigate this point, we set up 3D cultures of intestinal colonoids, which are a very useful model, as compared to established cell lines or primary 2D models, to study physiopathologic mechanisms of disease, although,

since they are composed of epithelial cells only, do not represent the complexity of pluricellular organisms.

In our experiments, colonoids were produced by using stem cells from the uninflamed colonic tissues of patients with UC. Undifferentiated colonoids were exposed to a mix of pro-inflammatory cytokines (TNFα and INFγ, denominated cytomix) to verify if they were able to respond to inflammatory agents. We found that colonoids were prone to develop inflammation by using a dose of cytomix not exceeding 150 ng/ml in order to avoid cytotoxicity. Colonoids, following the induction of inflammation, were also able to activate PARP1, as evidenced by the presence of the two cleaved forms of the protein (89 and 55 kDa). To analyze the release of HMGB1, colonoids were appropriately treated so as to recover the lumen content. The western blot analysis showed that secreted HMGB1 was significantly higher in the lumen of colonoids exposed to the cytomix. These results confirmed that gut colonoids derived from UC patients represent a suitable tool to investigate gut inflammation.

To assess the role of PARP1 in mediating the HMGB1 release, we treated colonoids with a PARP1-specific inhibitor, the PJ34, in addition to the cytomix. Thus, after selecting the right dose of PJ34 to be administered without incurring in cytotoxic effect, we co-exposed colonoids to cytomix and PJ34 or to cytomix alone and showed that the presence of PJ34

significantly inhibited the release of HMGB1 in the lumen. This finding confirms a strict relationship between PARP1 and HMGB1 during inflammation.

Furthermore, to stress the ability of PJ34 to alleviate inflammation, we also analysed the presence of other inflammatory markers, such as IL-1β, IL-8, and TNFα as well as that of the stress oxidative enzyme dual oxidase maturation factor 2 (DUOXA2). While the role of these cytokines in inflammation is well known, instead the role of DUOXA2 is less recognized. What is well known is that dual oxidases (DUOX) are conserved reduced nicotinamide adenine dinucleotide phosphate oxidases that produce H2O2 at the epithelial cell surface. The DUOX enzyme comprises the DUOX and DUOX maturation factor (DUOXA) subunits. Mammalian genomes encode 2 DUOX isoenzymes (DUOX1/DUOXA1 and DUOX2/DUOXA2). Recent data report that the expression of these genes is up-regulated during bacterial infections and chronic inflammatory diseases of the luminal gastrointestinal tract[148].

Moreover, it has been reported that both DUOX2 and DUOXA2 expression are involved specifically in inflammation and are regulated on a crypt-by-crypt basis in ulcerative colitis tissues[149].

We showed that PJ34 significantly reduced the mRNA expression of TNFα and DUOXA2 in colonoids exposed to cytomix.

All these results highlight the role of PARP1 inhibitor to improve gut inflammation.

Since the gut is mainly composed of differentiated cells, we induced the differentiation in colonoids taken from the stem cells of UC patients in order to better mimic the physiological condition. Once obtained, we exposed differentiated colonoids to different doses of cytomix to select the one less toxic but capable of inducing inflammation. We observed that both doses were able to induce inflammation without reducing cell viability, but only the higher dose of cytomix was able to induce a significant release of HMGB1. Thus, we choose this dose (150 ng/ml) in combination with three different doses of the PARP1 inhibitor PJ34 to verify its potential to decrease the inflammation also in differentiated colonoids. We observed that the two highest doses of PJ34 were toxic to colonoids, but the lower dose had no side effects and was able to significantly reduce the HMGB1 release in the lumen.

In conclusion, this research offers a novel evidence that PARP1 interacts with HMGB1 in controlling gut inflammation. Indeed, our results clearly show the link

between the two proteins to synergize and induce inflammatory processes.

Although PARP1 has been recognized as an important regulator of stress, inflammatory and numerous other cellular responses, its manipulation has only recently been identified as a strategy to control gut inflammation. By using animal models as well gut colonoid cultures, we undoubtly demonstrate that the strategy to impair PARP1 activity is a novel approach to manage gut inflammation decreasing the levels of inflammatory molecules and, after all, the release of the extracellular HMGB1 that is currently well accepted as a most potent inflammatory mediator.

Results obtained in this study open new perspectives on the relationship between PARP1 and the potent mediator HMGB1, focusing on the potential use of PARP1 inhibitors to manage IBD patients, after all those that do not respond to the tradional treatments.

7. REFERENCES

1. Zeng, Z., et al. From genetics to epigenetics, roles of epigenetics in inflammatory bowel disease. *Front. Genet.* **10**, 1–17 (2019).

2. Zhang, H., et al. Molecular diagnosis and classification of inflammatory bowel disease. *Expert Rev. Mol. Diagn.* **18**, 867–886 (2018).

3. Ventham, N. T., et al. Beyond gene discovery in inflammatory bowel disease: The emerging role of epigenetics. *Gastroenterology* **145**, 293–308 (2013).

4. Aleksandrova, K., et al. Diet, gut microbiome and epigenetics: Emerging links with inflammatory bowel diseases and prospects for management and prevention. *Nutrients* **9**, 1–13 (2017).

5. Kaplan, G. G. & Ng, S. C. Understanding and Preventing the Global Increase of Inflammatory Bowel Disease. *Gastroenterology* **152**, 313-321.e2 (2017).

6. Karatzas, P. S., et al. DNA methylation changes in inflammatory bowel disease. *Ann. Gastroenterol.* **27**, 125–132 (2014).

7. Yu, Y. R. & Rodriguez, J. R. Clinical presentation of Crohn's, ulcerative colitis, and indeterminate colitis: Symptoms, extraintestinal manifestations, and disease phenotypes. *Semin. Pediatr. Surg.* **26**, 349–355 (2017).

8. Tontini, G. E. et al. Differential diagnosis in inflammatory bowel disease colitis: State of the art and future perspectives. *World J. Gastroenterol.* **21**, 21–46 (2015).

9. Neurath, M. F. New targets for mucosal healing and therapy in inflammatory bowel diseases. *Mucosal Immunol.* **7**, 6–19 (2014).

10. de Lange, K. M. & Barrett, J. C. Understanding inflammatory bowel disease via immunogenetics. *Journal of*

Autoimmunity **64**, 91–100 (2015).

11. Raja, A. & Neurath, M. F. Current and Future Targets for Mucosal Healing in Inflammatory Bowel Disease. *Visc. Med.* **33**, 82–88 (2017).

12. Zhao, M & Burisch, J. Impact of Genes and the Environment on the Pathogenesis and Disease Course of Inflammatory Bowel Disease. *Dig Dis Sci.* **64**, 1759–1769 (2019).

13. Ananthakrishnan, A. N. Epidemiology and risk factors for IBD. *Nat. Rev. Gastroenterol. Hepatol.* **12**, 205–217 (2015).

14. Ellinghaus, D., et al. Association Between Variants of PRDM1 and NDP52 and Crohn's Disease, Based on Exome Sequencing and Functional Studies. *Gastroenterology* **145**, 339–347 (2013).

15. Liu, J. Z., et al. Association analyses identify 38 susceptibility loci for inflammatory bowel disease and highlight shared genetic risk across populations. *Nat Genet.* **47**, 979–986 (2015).

16. de Lange, K. M., et al. Genome-wide association study implicates immune activation of multiple integrin genes in inflammatory bowel disease. *Nat. Genet.* **49**, 256–261 (2017).

17. Huang, H., et al. Histone H3 trimethylation at lysine 36 guides m6 A RNA modification co-transcriptionally. *Nature* **567**, 414–419 (2019).

18. Yamashiro, Y. Gut Microbiota in Health and Disease. *Ann. Nutr. Metab.* **71**, 242–246 (2018).

19. Qin, J., et al. A human gut microbial gene catalog established by metagenomic sequencing. *Nature* **464**, 59–65 (2010).

20. Lloyd-Price, J., et al. Strains, functions, and dynamics in the expanded Human Microbiome Project. *Nature* **550**, 61–66 (2017).

21. Jandhyala S. M., et al. Role of the normal gut microbiota. *World J. Gastroenterol.* **21**, 8836–8847 (2015).

22. Sartor, R. B. Microbial Influences in Inflammatory Bowel Diseases. *Gastroenterology* **134**, 577–594 (2008).

23. Khan, I., et al. Alteration of Gut Microbiota in Inflammatory Bowel Disease (IBD): Cause or Consequence ? IBD Treatment Targeting the Gut Microbiome. *Pathogens* **8**, 1–28 (2019).

24. Gkouskou, K. K., et al. The gut microbiota in mouse models of inflammatory bowel disease. *Front. Cell. Infect. Microbiol.* **4**, 1–8 (2014).

25. Flint, H. J., et al. The role of the gut microbiota in nutrition and health. *Nat. Rev. Gastroenterol. Hepatol.* **9**, 577–589 (2012).

26. Bäumler, A.J. & Sperandio, V. Interactions between the microbiota and pathogenic bacteria in the gut. *Nature* **18**, 145–150 (2016).

27. Torow, N. & Hornef, M. W. The Neonatal Window of Opportunity: Setting the Stage for Life-Long Host-Microbial Interaction and Immune Homeostasis. *J. Immunol.* **198**, 557–563 (2017).

28. Arpaia, N., et al. Metabolites produced by commensal bacteria promote peripheral regulatory T cell generation. *Nature* **176**, 139–148 (2017).

29. Hooper, L. V. & MacPherson, A. J. Immune adaptations that maintain homeostasis with the intestinal microbiota. *Nat. Rev. Immunol.* **10**, 159–169 (2010).

30. Ivanov, I. I., et al. Induction of intestinal Th17 cells by segmented filamentous bacteria. *Cell* **139**, 485–498 (2009).

31. Lee, Y. K. & Mazmanian, S. K. Microbial learning lessons: SFB educate the immune system. *Immunity* **40**, 457–459 (2014).

32. Geuking, M. B., et al. Intestinal Bacterial Colonization Induces Mutualistic Regulatory T Cell Responses. *Immunity* **34**, 794–806 (2011).

33. Atarashi, K., et al. Treg induction by a rationally selected mixture of Clostridia strains from the human microbiota. *Nature* **500**, 232–236 (2013).

34. Mucida, D., et al. Reciprocal TH17 and regulatory T cell differentiation mediated by retinoic acid. *Science (80-.).* **317**, 256–60 (2007).

35. Round, J. L. & Mazmanian, S. K. Inducible Foxp3+ regulatory T-cell development by a commensal bacterium of the intestinal microbiota. *Proc. Natl. Acad. Sci. U. S. A.* **107**, 12204–12209 (2010).

36. Qiu, X., et al. Faecalibacterium prausnitzii upregulates regulatory T cells and anti-inflammatory cytokines in treating TNBS-induced colitis. *J. Crohn's Colitis* **7**, e558–e568 (2013).

37. Ni, J., et al. Gut microbiota and IBD: causation or correlation? *Nat Rev Gastroenterol Hepatol* **14**, 573–584 (2017).

38. Aggeletopoulou, I., et al. The role of the gut microbiota in the treatment of inflammatory bowel diseases. *Microb Pathog.* **137**, 103774 (2019).

39. Flach, M. & Diefenbach, A. Development of gut-associated lymphoid tissues. in *Mucosal Immunology, 4th Edn.* 31–42 (2015).

40. De Souza, H. S.P. & Fiocchi, C. Immunopathogenesis of IBD: current state of the art. *Nat. Rev. Gastroenterol. Hepatol.* 13–27 (2016). doi:10.1038/nrgastro.2016.186

41. Atreya, R. & Neurath, M. F. Factors Affecting Mucosal Homeostasis: A Fine Balance. in *Inflammatory Bowel Disease: Translating basic science into clinical practice* 52–63 (2010).

42. Peterson, L. W. & Artis, D. Intestinal epithelial cells: Regulators of barrier function and immune homeostasis. *Nat. Rev. Immunol.* **14**, 141–153 (2014).

43. Ahluwalia, B., et al. Immunopathogenesis of inflammatory bowel disease and mechanisms of biological therapies. *Scand. J. Gastroenterol.* **53**, 379–389 (2018).

44. Geremia, Al., et al. Innate and adaptive immunity in inflammatory bowel disease. *Autoimmun. Rev.* **13**, 3–10 (2014).

45. Masayuki, S., et al. High Frequency Haplotypes in the X Chromosome Locus TLR8 are Associated with Both CD and UC in Females Masayuki. *Inflamm Bowel Dis.* **15**, 321–327 (2009).

46. Henckaerts, L. & Vermeire, S. NOD2/CARD15 disease associations other than Crohn's disease. *Inflamm. Bowel Dis.* **13**, 235–241 (2007).

47. Torok, H.P., et al. Crohn's disease is associated with a toll-like receptor-9 polymorphism. *Gastroenterology.* **127**, 365–366 (2004).

48. Hart, A. L., et al. Characteristics of intestinal dendritic cells in inflammatory bowel diseases. *Gastroenterology* **129**, 50–65 (2005).

49. Middel, P., et al. Increased number of mature dendritic cells in Crohn's disease: Evidence for a chemokine mediated retention mechanism. *Gut* **55**, 220–227 (2006).

50. Neurath, M. F. Cytokines in inflammatory bowel disease. *Nat Rev Immunol.* **14**, 329–42 (2014).

51. Levin, A. D. et al. Mechanism of action of anti-TNF therapy in inflammatory bowel disease. *J. Crohn's Colitis* **10**, 989–997 (2016).

52. Rose-John, S. Il-6 trans-signaling via the soluble IL-6 receptor: Importance for the proinflammatory activities of IL-6. *Int. J. Biol. Sci.* **8**, 1237–1247 (2012).

53. Xavier, R. J. & Podolsky, D. K. Unravelling the pathogenesis of inflammatory bowel disease. *Nature* **448**, 427–434 (2007).

54. Rimoldi, M., et al. Intestinal immune homeostasis is regulated by the crosstalk between epithelial cells and dendritic cells. *Nat. Immunol.* **6**, 507–514 (2005).

55. Zhou, L., et al. Plasticity of CD4+ T Cell Lineage Differentiation. *Immunity* **30**, 646–655 (2009).

56. Fuss, I. J., et al. Disparate CD4+ lamina propria (LP) lymphokine secretion profiles in inflammatory bowel disease. Crohn's disease LP cells manifest increased secretion of IFN- gamma, whereas ulcerative colitis LP cells manifest increased secretion of IL-5. *J Immunol.* **157**, 1261–1270 (1996).

57. Heller, F., et al. Interleukin-13 is the key effector Th2 cytokine in ulcerative colitis that affects epithelial tight junctions, apoptosis, and cell restitution. *Gastroenterology* **129**, 550–564 (2005).

58. Fuss, I. J. & Stober, W. The role of IL-13 and NK T cells in experimental and human ulcerive colitis. *Mucosal Immunol.* **1**, S31–S33 (2008).

59. Neurath, M. F. Targeting immune cell circuits and trafficking in inflammatory bowel disease. *Nat. Immunol.* **20**, 970–979 (2019).

60. Shouval, D. S. & Rufo, P. A. The role of environmental factors in the pathogenesis of inflammatory bowel diseases: a review. *JAMA Pediatr* **171**, 999–1005 (2017).

61. Ng, S. C., et al. Worldwide incidence and prevalence of inflammatory bowel disease in the 21st century: a systematic review of population-based studies. *Lancet* **390**, 2769–2778 (2017).

62. Khor, B. et al. Genetics and pathogenesis of IBD. *Nature* **474**, 307–317 (2011).

63. Allais, L., et al. Chronic cigarette smoke exposure induces microbial and inflammatory shifts and mucin changes in the murine gut. *Environ. Microbiol.* **18**, 1352–1363 (2016).

64. Hou, J. K., et al. Dietary intake and risk of developing inflammatory bowel disease: A systematic review of the literature. *Am. J. Gastroenterol.* **106**, 563–573 (2011).

65. Ananthakrishnan, A. N., et al. Long-term intake of dietary fat and risk of ulcerative colitis and Crohn's disease. *Gut* **63**, 776–784 (2014).

66. Shaw, S. Y., et al. Association between the use of antibiotics in the first year of life and pediatric inflammatory bowel disease. *Am. J. Gastroenterol.* **105**, 2687–2692 (2010).

67. Selby, W., et al. Two-Year Combination Antibiotic Therapy With Clarithromycin, Rifabutin, and Clofazimine for Crohn's Disease. *Gastroenterology* **132**, 2313–2319 (2007).

68. Olszak, T., et al. Microbial Exposure During Early Life Has Persistent Effects on Natural Killer T Cell Function. *Science (80-.).* **336**, 489–493 (2012).

69. Khalili, H., et al. Oral contraceptives, reproductive factors and risk of inflammatory bowel disease. *Gut* **62**, 1153–1159 (2013).

70. Ananthakrishnan, A. N., et al. Aspirin, Nonsteroidal Anti-inflammatory Drug Use, and Risk for Crohn Disease Ulcerative Colitis: A Cohort Study. *Ann Intern Med.* **156**, 350–359 (2012).

71. Ng, S. C., et al. Environmental risk factors in inflammatory bowel disease: A population-based case-control study in Asia-Pacific. *Gut* **64**, 1063–1071 (2015).

72. Chu, K. M., et al. Childhood helminth exposure is protective against inflammatory bowel disease: A case control study in South Africa. *Inflamm. Bowel Dis.* **19**, 614–620 (2013).

73. Bager, P., et al. Cesarean section and offspring's risk of inflammatory bowel disease: a national cohort study.

Inflamm Bowel Dis. **18**, 857–862 (2012).

74. Thoo, L., et al. Keep calm: the intestinal barrier at the interface of peace and war. *Cell Death Dis.* **10**, 849 (2019).

75. Artis, D. Epithelial-cell recognition of commensal bacteria and maintenance of immune homeostasis in the gut. *Nat. Rev. Immunol.* **8**, 411–420 (2008).

76. Chen, G. Y. & Nuñez, G. Sterile inflammation: Sensing and reacting to damage. *Nat. Rev. Immunol.* **10**, 826–837 (2010).

77. Andrews, C., et al. Cytokine tuning of intestinal epithelial function. *Front. Immunol.* **9**, (2018).

78. Sato, T., et al. Paneth cells constitute the niche for Lgr5 stem cells in intestinal crypts. *Nature* **469**, 415–418 (2011).

79. Nieuwenhuis, E. E. & Blumberg, R. S. The role of the epithelial barrier in inflammatory bowel disease. *Adv Exp Med Biol* **579**, 106–16 (2006).

80. Štros, M. HMGB proteins: Interactions with DNA and chromatin. *Biochim. Biophys. Acta - Gene Regul. Mech.* **1799**, 101–113 (2010).

81. Bustin, M. Revised nomenclature for high mobility group (HMG) chromosomal proteins. *Trends Biochem Sci* **26**, 152–3 (2001).

82. Kozlova, A. L., et al. HMGB Proteins as DNA Chaperones That Modulate Chromatin Activity. *Mol. Biol.* **52**, 637–647 (2018).

83. Reeves, R. HMG Nuclear Proteins: Linking Chromatin Structure to Cellular Phenotype. *Biochim. Biophys. Acta - Gene Regul. Mech.* **1799**, 3–14 (2010).

84. Jung, Y. & Lippard, S. J. Nature of full-length HMGB1 binding to cisplatin-modified DNA. *Biochemistry* **11**, 2664–71 (2003).

85. Štros, M. DNA bending by the chromosomal protein HMG1

and its high mobility group box domains: Effect of flanking sequences. *J. Biol. Chem.* **273**, 10355–10361 (1998).

86. Blair, R. H., et al. The HMGB1 C-terminal tail regulates DNA bending Rebecca. *J Mol Biol.* **428**, 4060–4072 (2016).

87. Matzinger, P. The danger model: A renewed sense of self. *Science (80-.).* **296**, 301–305 (2002).

88. Piccinini, A. M. & Midwood, K. S. DAMPening inflammation by modulating TLR signalling. *Mediators Inflamm.* **2010**, (2010).

89. Andersson, U. & Tracey, K. T. HMGB1 Is a Therapeutic Target for Sterile Inflammation and Infection. *Annu Rev Immunol.* **29**, 139–162 (2011).

90. Harris, H. E., et al. HMGB1: A multifunctional alarmin driving autoimmune and inflammatory disease. *Nat. Rev. Rheumatol.* **8**, 195–202 (2012).

91. Lu, B., et al. JAK/STAT1 signaling promotes HMGB1 hyperacetylation and nuclear translocation. *Proc. Natl. Acad. Sci. U. S. A.* **111**, 3068–3073 (2014).

92. Yang, H., et al. The many faces of HMGB1: molecular structure-functional activity in inflammation, apoptosis, and chemotaxis. *J. Leukoc. Biol.* **93**, 865–873 (2013).

93. Andersson, U., et al. Extracellular HMGB1 as a therapeutic target in inflammatory diseases. *Expert Opin Ther Targets.* **22**, 263–277 (2018).

94. Hu, Z., et al. Role of high-mobility group box 1 protein in inflammatory bowel disease. *Inflamm. Res.* **64**, 557–563 (2015).

95. Pellegrini, L., et al. HMGB1 and repair: focus on the heart. *Pharmacol Ther.* **196**, 160–182 (2019).

96. Paudel, Y. N. et al. Enlightening the role of high mobility group box 1 (HMGB1) in inflammation: Updates on receptor signalling. *Eur. J. Pharmacol.* **858**, 172487 (2019).

97. Kang, R., et al. HMGB1 in cancer: Good, bad, or both? *Clin. Cancer Res.* **19**, 4046–4057 (2013).

98. Bianchi, M. E. HMGB1 loves company. *J. Leukoc. Biol.* **86**, 573–576 (2009).

99. Xu, T., et al. The progression of HMGB1-induced autophagy in cancer biology. *Onco. Targets. Ther.* **12**, 365–377 (2019).

100. Yamasaki, H., et al. Roles of high-mobility group box 1 in murine experimental colitis. 23–27 (2009). doi:10.3892/mmr

101. Lin, L., et al. HMGB1 contributes to the development of acute murine colitis. *Chin J Dig Endosc.* 247 (2009).

102. Dave, S. H., et al. Ethyl pyruvate decreases HMGB1 release and ameliorates murine colitis. **86**, 633–643 (2009).

103. Chen, X., et al. HMGB1 exacerbates experimental mouse colitis by enhancing innate lymphoid cells 3 inflammatory responses via promoted IL-23 production. *Innate Immun.* **22**, 696–705 (2016).

104. Vitali, R., et al. Dipotassium Glycyrrhizate Inhibits HMGB1-Dependent Inflammation and Ameliorates Colitis in Mice. *PLoS One* **8**, (2013).

105. Stronati, L., et al. Dipotassium glycyrrhizate improves intestinal mucosal healing by modulating extracellular matrix remodeling genes and restoring epithelial barrier functions. *Front. Immunol.* **10**, 1–14 (2019).

106. Palone, F., et al. Fecal HMGB1 Reveals Microscopic Inflammation in Adult and Pediatric Patients with Inflammatory Bowel Disease in Clinical and Endoscopic Remission. **22**, 2886–2893 (2016).

107. Bock, F. J. & Chang, P. New directions in poly(ADP-ribose) polymerase biology. *FEBS J.* **283**, 4017–4031 (2016).

108. Gupte, R., et al. Parps and adp-ribosylation: Recent advances linking molecular functions to biological outcomes.

Genes Dev. **31**, 101–126 (2017).

109. Gibson, B.A. & Kraus, W. L. New insights into the molecular and cellular functions of poly(ADP- ribose) and PARPs. *Nat. Rev. Mol. Cell Biol.* **13**, 411–424 (2012).

110. Luo, X. & Kraus Lee, W. On par with PARP: Cellular stress signaling through poly(ADP-ribose) and PARP-1. *Genes Dev.* **26**, 417–432 (2012).

111. Ke, y., et al. The Role of PARPs in Inflammation—and Metabolic—Related Diseases: Molecular Mechanisms and Beyond. *Cells* **8**, 1047 (2019).

112. Bork, P., et al. A superfamily of conserved domains in DNA damage-responsive cell cycle checkpoint proteins. *FASEB J.* **11**, 68–76 (1997).

113. Li, N. & Chen, J. ADP-Ribosylation: Activation, Recognition, and Removal. *Mol. Cells* **37**, 9–16 (2014).

114. Lonskaya, I., et al. Regulation of poly(ADP-ribose) polymerase-1 by DNA structure-specific binding. *J. Biol. Chem.* **280**, 17076–17083 (2005).

115. Rock, K. L. & Kono, H. The inflammatory response to cell death. *Annu Rev Pathol.* **3**, 99–126 (2008).

116. Elliott, R.B., et al. The use of nicotinamide in the prevention of type 1 diabetes. *Ann NY Acad Sci* **696**, 333–341 (1993).

117. Giansanti, V., et al. PARP inhibitors: new tools to protect from inflammation. *Biochem Pharmacol* **80**, 1869–1877 (2010).

118. Oliver, F. J., et al. Resistance to endotoxic shock as a consequence of defective NF-κB activation in poly (ADP-ribose) polymerase-1 deficient mice. *EMBO J.* **18**, 4446–4454 (1999).

119. Hassa, P. O. & Hottiger, M. O. A role of poly (ADP-Ribose) polymerase in NF-κB transcriptional activation. *Biol. Chem.* **380**, 953–959 (1999).

120. Chen, Z., et al. Signal-induced site-specific phosphorylation targets IκBα to the ubiquitin-proteasome pathway. *Genes Dev.* **9**, 1586–1597 (1995).

121. Valdor, R., et al. Regulation of NFAT by poly(ADP-ribose) polymerase activity in T cells. *Mol. Immunol.* **45**, 1863–1871 (2008).

122. Yang, Z., et al. PARP-1 Mediates LPS-Induced HMGB1 Release by Macrophages through Regulation of HMGB1 Acetylation. *J Immunol* **193**, 6114–6123 (2014).

123. Davis, K., et al. Poly(ADP-Ribosyl)ation of high mobility group box 1 (HMGB1) protein enhances inhibition of efferocytosis. *Mol. Med.* **18**, 359–369 (2012).

124. Ye, T. J., et al. High mobility group box-1 release from H2O2-injured hepatocytes due to sirt1 functional inhibition. *World J. Gastroenterol.* **25**, 5434–5450 (2019).

125. Peralta-Leal, A., et al. PARP inhibitors: New partners in the therapy of cancer and inflammatory diseases. *Free Radic. Biol. Med.* **47**, 13–26 (2009).

126. Larmonier, C. B., et al. Transcriptional Reprogramming and Resistance to Colonic Mucosal Injury in Poly (ADP-ribose) Polymerase 1 (PARP1) - deficient Mice. *J. Biol. Chem.* **291**, 8918–8930 (2016).

127. Cuzzocrea, S., et al. Role of poly(ADP-ribose) glycohydrolase in the development of inflammatory bowel disease in mice. *Free Radic. Biol. Med.* **42**, 90–105 (2007).

128. Jijon, H. B., et al. Inhibition of poly(ADP-ribose) polymerase attenuates inflammation in a model of chronic colitis. *Am J Physiol Gastrointest Liver Physiol* 641–651 (2000).

129. Di Paola, R., et al. Treatment with PARP-1 inhibitors, GPI 15427 or GPI 16539, ameliorates intestinal damage in rat models of colitis and shock. *Eur. J. Pharmacol.* **527**, 163–171 (2005).

130. Mabley, J. G., et al. Anti-inflammatory effects of a novel , potent inhibitor of poly. *Inflamm. Res.* **50**, 561–569 (2001).

131. Zingarelli B., O'Connor M., and H. P. W. Inhibitors of poly (ADP-ribose) polymerase modulate signal transduction pathways in colitis. ; *Eur. J. Pharmacol.* 183–184 (2003).

132. Zingarelli, B., et al. Activator protein-1 signalling pathway and apoptosis are modulated by poly(ADP-ribose) polymerase-1 in experimental colitis. *Immunology* **113**, 509–517 (2004).

133. Huang, F. C. Upregulation of salmonella-induced IL-6 production in caco-2 cells by PJ-34, parp-1 inhibitor: Involvement of PI3K, p38 MAPK, ERK, JNK, and NF- B. *Mediators Inflamm.* (2009).

134. Sato, T., et al. Single Lgr5 stem cells build crypt – villus structures in vitro without a mesenchymal niche. *Nature* **459**, 262–265 (2009).

135. Jung, P., et al. Isolation and in vitro expansion of human colonic stem cells. *Nat. Med.* **17**, 1225–1227 (2011).

136. Takahashi T. Organoids for Drug Discovery and Personalized Medicine. *Pharmacol Toxicol. Annu Rev* 447–462 (2019).

137. Grabinger, T., et al. Ex vivo culture of intestinal crypt organoids as a model system for assessing cell death induction in intestinal epithelial cells and enteropathy. *Cell Death Dis.* **5**, e1228-10 (2014).

138. Lesuffleur, T., et al. Differential expression of the human mucin genes MUC1 to MUC5 in relation to growth and differentiation of different mucus-secreting HT-29 cell subpopulations. *J. Cell Sci.* **106**, 771–783 (1993).

139. Sambuy, Y., et al. The Caco-2 cell line as a model of the intestinal barrier: Influence of cell and culture-related factors on Caco-2 cell functional characteristics. *Cell Biol. Toxicol.* **21**, 1–26 (2005).

140. Howitt, M. R., et al. Tuft cells, taste-chemosensory cells, orchestrate parasite type 2 immunity in the gut. *Science (80-.).* **351**, 1329–1333 (2016).

141. Bellono, N. W., et al. Enterochromaffin cells are gut chemosensors that couple to sensory neural pathway. *Cell* **170**, 185–198 (2017).

142. Foulke-Abel, J., et al. Human enteroids as an ex-vivo model of host–pathogen interactions in the gastrointestinal tract. *Exp Biol Med* **239**, 1124–1134 (2014).

143. Suzuki, K., et al. Single cell analysis of Crohn's disease patient-derived small intestinal organoids reveals disease activity-dependent modification of stem cell properties. *J. Gastroenterol.* **53**, 1035–1047 (2018).

144. Howell, K. J., et al. DNA Methylation and Transcription Patterns in Intestinal Epithelial Cells From Pediatric Patients With Inflammatory Bowel Diseases Differentiate Disease Subtypes and Associate With Outcome. *Gastroenterology* **154**, 585–598 (2018).

145. Holmberg, F. E., et al. Culturing human intestinal stem cells for regenerative applications in the treatment of inflammatory bowel disease. *EMBO Mol. Med.* **9**, 558–570 (2017).

146. Maxwell, J.R., et al. Methods of inducing inflammatory bowel disease in mice. *Curr. Protoc. Pharmacol.* **5**, 1–5 (2009).

147. Lukovac, S. & Roeselers, G. Intestinal Crypt Organoids as Experimental Models. in *The Impact of Food Bioactives on Health* 245–254 (2015).

148. Grasberger, H., et al. Dual Oxidases Control Release of Hydrogen Peroxide by the Gastric Epithelium to Prevent Helicobacter felis Infection and Inflammation in Mice. *Gastroenterology* **145**, 1045–1054 (2013).

149. MacFie, T. S., et al. DUOX2 and DUOXA2 form the predominant enzyme system capable of producing the

reactive oxygen species H2O2 in active ulcerative colitis and are modulated by 5-aminosalicylic acid. *Inflamm. Bowel Dis.* **20**, 514–524 (2014).